GLI2 is a regulator of β-catenin and is associated with loss of E-cadherin, cell invasiveness and long-term epidermal regeneration

Eleni Pantazi[1], Emilios Gemenetzidis[1], Muy-Teck Teh[2], Sreekanth Vootukuri Reddy[1], Gary Warnes[3], Chris Evagora[4], Giuseppe Trigiante[1] and Michael P. Philpott[1+].

[1] Centre

for Cell Biology and Cutaneous Research, Blizard Institute, Barts and The London School of Medicine and Dentistry, Queen Mary University of London, London, United Kingdom.

[2] Department of Diagnostic and Oral Sciences, Blizard Institute, Barts and The London School of Medicine and Dentistry, Queen Mary University of London, London, United Kingdom.

[3] Imaging and Flow Cytometry Core facilities, Blizard Institute, Barts and The London School of Medicine and Dentistry, Queen Mary University of London, London, United Kingdom.

[4] Pathology Core facilities, Blizard Institute, Barts and The London School of Medicine and Dentistry, Queen Mary University of London, London, United Kingdom.

[+]Corresponding author:

Centre for Cell Biology and Cutaneous Research, Blizard Institute, Barts and The London School of Medicine and Dentistry, Queen Mary University of London, 4 Newark Street, London, E1 2AT, United Kingdom. Phone: +44 207 882 7162 Fax: +44 207 882 7171

Email m.p.philpott@qmul.ac.uk

Running Title: GLI2 regulates β-catenin and cell invasion

Financial Support: This work was supported by grant DERG1D8R from Research Advisory Board of the Barts and the London Charity.

Conflict of interest: The authors state no conflict of interest.

Abstract

Uncontrolled HH/GLI and WNT/β-catenin signaling are important events in the genesis of many cancers including skin cancer and are often implicated in tumour progression, invasion and metastasis. However, due to the complexity and context-dependency of both pathways, little is known about HH and WNT interactions in human carcinogenesis. In the current study we provide evidence of HH/GLI2-WNT/β-catenin signaling crosstalk in human keratinocytes. Over-expression of GLI2ΔN in human keratinocytes resulted in cytoplasmic accumulation and nuclear relocalization of β-catenin *in vitro* and in 3D-organotypic cultures, accompanied by upregulation of WNT genes. Induction of GLI2ΔN, enhanced the β-catenin-dependent transcriptional activation and the subsequent activation of β-catenin target genes including Cyclin-D1. Additionally, GLI2 overexpression was associated with decreased E-cadherin protein levels, increased expression of SNAIL, MMP2 and integrin β1, and with increased cell invasion in 3D-organotypic cultures. Invasion was reduced by Wnt inhibition, thus unveiling direct role of GLI2/Wnt crosstalk in cell invasion. We also showed that GLI2 supported long-term epidermal regeneration in 3D-organotypic cultures and induced an undifferentiated basal/stem cell-associated phenotype, in line with the role of β-catenin and SNAIL in epidermal stem cell maintenance. This work suggests that GLI2 is a regulator of β-catenin and provides insights into its role in tumourigenesis.

Keywords

keratinocytes, BCC, GLI2, β-catenin, HH, WNT, invasion, E-cadherin

Introduction

The Hedgehog (HH) signaling pathway is highly conserved in embryonic development, while its constitutive activation is implicated in basal cell carcinomas (BCCs), medulloblastomas, glioma and rhabdosarcoma development (Aberger and Ruiz, 2014, Beachy et al. , 2004, Gorlin, 1995, Ruiz i Altaba et al. , 2002). GLI2 is the key transcriptional effector of the HH pathway and probably the major mediator of malignant transformation induced by the loss of PTCH1 in BCC (Li et al. , 2014, Pantazi et al. , 2014, Yin et al. , 2015).

GLI2 up-regulation is frequently observed in human BCCs (Ikram et al. , 2004, O'Driscoll et al. , 2006, Regl et al. , 2004b, Tojo et al. , 2003), while its targeted constitutive overexpression in transgenic mice causes BCC formation and is required for BCC maintenance (Grachtchouk et al. , 2000, Hutchin et al. , 2005). GLI2 is also consistently up-regulated in aggressive cancers (Ruiz i Altaba, Sanchez, 2002, Thiyagarajan et al. , 2007, Zhang et al. , 2013) and is associated with invasion and metastasis (Alexaki et al. , 2010, Javelaud et al. , 2011, Marsh et al. , 2008, Snijders et al. , 2008, Sterling et al. , 2006). Using an *in vitro* model of human BCC, we showed that GLI2 suppresses cell cycle regulators, inhibits apoptosis, and induces genomic instability (Pantazi, Gemenetzidis, 2014).

B-catenin is the major and downstream effector of the canonical WNT signaling pathway (Behrens et al. , 1996). Transactivation of WNT target genes have been linked to tumor formation, invasion and metastasis (Marchenko et al. , 2002, Polakis, 2000). In mice,

β-catenin controls hair follicle morphogenesis and stem cell differentiation (Huelsken et al. , 2001), while its inappropriate activation promotes the formation of follicle and BCC-like tumors (Gat et al. , 1998, Nicolas et al. , 2003).

HH/GLI2-driven human BCCs show increased levels of WNT genes such as WNT2B, WNT5A, WNT7A and WNT11 (Bonifas et al. , 2001, Mullor et al. , 2001, O'Driscoll, McMorrow, 2006, Saldanha et al. , 2004, Yu et al. , 2008), accumulation of cytoplasmic and nuclear β-catenin (El-Bahrawy et al. , 2003, Papanikolaou et al. , 2010, Saldanha, Ghura, 2004, Yamazaki et al. , 2001, Yang et al. , 2008) and increased mRNA levels of the matrix metalloproteinases (MMP), which are known targets of β-catenin-TCF/LEF-1 signaling (O'Driscoll, McMorrow, 2006, Sternlicht et al. , 1999, Yu, Zloty, 2008).

Due to the complexity and context-dependency of both HH and WNT pathways little is known about HH and WNT interactions in human carcinogenesis. In the current study we provide evidence of HH/GLI2-WNT/β-catenin signaling crosstalk in human keratinocytes. Over-expression of GLI2ΔN in N/TERT human keratinocytes, promotes nuclear relocalization and enhanced transcriptional activation of β-catenin, as well as loss of E-cadherin protein expression, increased SNAIL, MMP2 and integrin β1 expression, increased cell invasion and long-term epidermal regeneration in organotypic cultures. We propose that GLI2 is a regulator of β-catenin and provide insights into its role in carcinogenesis and tumour progression.

Results

GLI2ΔN promotes nuclear re-localization of β-catenin and induces β-catenin dependent transactivation in human keratinocytes

B-catenin re-localization to the nucleus is a necessary step for the transcriptional activation of its downstream genes and is tightly controlled. To investigate whether GLI2ΔN expression can alter the sub-cellular distribution of β-catenin control N/TERT EGFP (SINCE) and EGFP-GLI2ΔN (SINEG2)-expressing keratinocytes were seeded at equal densities and harvested for cytoplasmic and nuclear protein fractions. Increased nuclear and decreased cytoplasmic β-catenin, was observed in SINEG2 cells compared to SINCE keratinocytes (Figure 1a, b, d), Overall levels of β-catenin were similar in both SINCE and SINEG2 keratinocytes (Figure 1c).

To investigate whether the increased nuclear β-catenin is transcriptionally active, we used (Supplementary Materials and Methods) the well characterized OT-β-catenin responsive promoter (OT), an improved version of TOPFLASH (Shih et al. , 2000). GLI2ΔN-expressing keratinocytes showed a significant increase in the transactivation of β-catenin compared to N/TERT and SINCE control cells (Figure 1e). Cyclin-D1, a β-catenin-regulated gene (Shtutman et al. , 1999, Tetsu and McCormick, 1999) was also upregulated (Supplementary Figure S1).

We confirmed these data using inducible GLI2ΔN-expressing keratinocytes (NTEG2) (see Supplementary Material Methods, Supplementary Results, Supplementary Figure S2, S3a). B-catenin transcriptional activation was significantly increased in

NTEG2 (Dox-) keratinocytes compared to both NTEG2 (Dox+) and N/TERT control cells (Supplementary Figure S3b). Immunoblotting for EGFP and active β-catenin (Supplementary Figure S3c) showed that active β-catenin was significantly higher in the induced NTEG2 cells compared to control cells.

Induction of multiple WNT ligands upon GLI2ΔN expression in N/TERT keratinocytes

WNT genes are activated during embryonic development upon Gli2 induction and in human BCCs (Bonifas, Pennypacker, 2001, Mullor, Dahmane, 2001, Yu, Zloty, 2008), where GLI2 is highly expressed.

Stable expression of GLI2ΔN in human keratinocytes resulted in the upregulation of WNT5A (Figure 2a), WNT7A (Figure 2b) and WNT11 (Figure 2c), compared to wild-type and EGFP-expressing N/TERT keratinocytes. The relative fold mRNA induction of WNT11 could be an overestimation, due to the very low background levels of WNT11 mRNA observed in control N/TERT and SINCE keratinocytes (Ct >31).

Stable GLI2ΔN expression in N/TERT keratinocytes induces downregulation of E-cadherin protein expression and upregulation of EMT markers

Immunoblotting analysis showed a significant reduction of E-cadherin in SINEG2 cells, compared to control N/TERT and SINCE keratinocytes (Figure 3a). Loss of E-cadherin is believed to promote loss of cell-cell adhesion and release of the membranous β-catenin to the cytoplasm (Canel et al. , 2013), and is associated with epithelial-mesenchymal

transitions (EMT) both during development and during tumour progression (Cavallaro and Christofori, 2004, Hugo et al. , 2007, Nelson and Nusse, 2004, Thiery, 2002). The EMT markers SNAIL1 and SNAIL2 both suppress E-cadherin (Batlle et al. , 2000, Hajra et al. , 2002). We showed by quantitative real-time PCR (qRT-PCR) analysis that stable expression of GLI2ΔN in human N/TERT keratinocytes, results in up-regulation of SNAIL1 (Figure 3b), and to a lesser extent of SNAIL2 (Figure 3c). The levels E-cadherin mRNA remained unchanged (Figure 3d), despite E-cadherin protein down-regulation (Figure 3a), suggesting that the down-regulation of E-cadherin protein in SINEG2 cells might be a result of post-translational processes.

Increased capacity of GLI2ΔN-expressing cells to invade collagen/matrigel gels

Nuclear active β-catenin, loss of E-cadherin and up-regulation of both WNT and SNAIL, are implicated in cancer cell invasion and metastasis. Haematoxylin and eosin (H&E) (Figure 4a), cytokeratin and DAPI staining (Figure 4b) showed that N/TERT and SINCE controls produced a stratified epithelium with no cell invasion (Figure 4a and Figure 4b). In contrast, SINEG2 cells, produced a thicker, poorly differentiated epithelium with clusters of basal-like cells invading into the upper region of the collagen layer, recapitulating the histopathology of nodular and superficial human BCC. SINEG2 cells also invaded as protrusive multicellular strands with a blunt bud-like tip that remained in connection with the overlying epidermis (Figure 4b; SINEG2 panels), similar to hair follicle bud formation. Cytokeratin staining (red) of the epithelium was uniform in all organotypics (Figure 4b). Quantification of invasive cells (as described in materials and

methods) showed that SINEG2 keratinocytes were significantly more invasive compared to control cells (Figure 4c).

MMP2, which is a known target of β-catenin-TCF/LEF-1 (Wu et al. , 2007), was significantly increased mRNA levels, as shown by qRT-PCR, and protein levels, as shown by MPP2 staining in SINEG2 organotypic cultures especially at the periphery of invading multicellular strands and clusters (Supplementary Figure S4a, b). We then repeated the organotypic cultures for a period of 14 days, with continuous treatment of human recombinant sFRP-1, which acts as an antagonist of WNT signaling. Although SINEG2 cells treated with sFRP-1 produced a similar basal-like undifferentiated epithelium, cells displayed a reduced capacity for invasion into the organotypic ECM (Figure S5).

Loss of membranous E-cadherin and β-catenin expression in GLI2ΔN organotypic cultures

Loss and/or fragmentation of membranous E-cadherin and β-catenin, as well as altered cellular distribution of β-catenin were also observed in organotypic cultures of GLI2ΔN-expressing cells at 14 days, supporting our immunoblotting data. Immunohistochemistry for E-cadherin, showed strong and complete membranous expression in SINCE control cells (Figure 5a). However, E-cadherin staining was fragmented or lost in SINEG2 cells in the upper epithelium as well as in invading cells, and especially at the periphery of invading cells (Figure 5a; SINEG2 panels). Immunohistochemistry for β-catenin showed strong continuous membranous staining in

SINCE control cells, while SINEG2 cells exhibited partial or complete loss of membranous β-catenin staining (Figure 5b, c). This pattern was associated with weak diffuse cytoplasmic and/or focally nuclear staining in SINEG2 cells, and was observed both in the upper epithelium, as well as in the invading GLI2ΔN-expressing cells, with only few cells retaining the membranous β-catenin stain.

GLI2ΔN-expressing cells support long-term epidermal regeneration in organotypic cultures and display an undifferentiated basal stem-cell like phenotype *in vitro*

Prolonged culture of N/TERT and SINCE organotypic for 28 days showed marked epidermal atrophy (Figure 6a, b), which is consistent with the limited regenerative potential of keratinocytes grown on a collagen gels (Muffler et al. , 2008, Stark et al. , 1999). In contrast, SINEG2 cells retained a stratified epithelium at 28 days (Figure 6a; b), and maintained the capacity for deep invasion into the ECM (Figure 6c-e)

Lack of atrophy in GLI2ΔN keratinocytes may be due to impaired differentiation, and/or due to maintenance of a basal/stem cell phenotype. This was confirmed *in vitro* by the down-regulation of involucrin in SINEG2 cells (Figure 6f), as well as of c-MYC (Figure 6g, j), which is another marker of keratinocyte differentiation (Gandarillas and Watt, 1997). Integrin β1, a marker for the enrichment of epidermal keratinocyte stem cells (Jones et al. , 1995, Jones and Watt, 1993, Zhu et al. , 1999), was increased in SINEG2 keratinocytes compared to control cells (Figure 6h). Similar changes have been reported in human BCCs (Daya-Grosjean and Couve-Privat, 2005, Miller, 1991, O'Driscoll, McMorrow, 2006, Youssef et al. , 2010). Finally, SOX2 a well-characterized

stem cell associated gene (Fong et al. , 2008, Masui et al. , 2007, Niwa, 2007), was markedly up-regulated in SINEG2 keratinocytes, compared to controls (Figure 6i), although the relative fold mRNA induction could have been overestimated due to the low SOX2 mRNA copy number in control keratinocytes (Ct >31).

Discussion

The HH and WNT pathways play pivotal roles in development and stem cell maintenance and are implicated in the etiology of a range of cancers including BCC. The crosstalk between these pathways has not been fully investigated in human cells, although targeted inhibition makes them attractive therapeutic targets. Here we provide evidence of HH/GLI2 crosstalk with the WNT/β-catenin pathway in human keratinocytes and more evidence for the role of GLI2 in key aspects of tumourigenesis. Overexpression of the constitutively active form of GLI2 (GLI2ΔN), in N/TERT human epidermal keratinocytes, promoted cytoplasmic accumulation and nuclear re-localization of β-catenin, and enhanced its transcriptional activation. This was associated with loss of E-cadherin protein expression, cell invasion and long-term epidermal regeneration in organotypic cultures.

β-catenin, the downstream mediator of the Wnt pathway, is usually confined to the cell membrane in an adhesion complex including E-cadherin (Nelson and Nusse, 2004). Its cytoplasmic concentration in the absence of WNT activation remains low and its nuclear relocalization and transcriptional activity is tightly regulated. Activation of β-catenin is

strongly implicated in carcinogenesis, invasion, EMT, and metastasis (Brabletz et al. , 2005, Kim et al. , 2002, Klaus and Birchmeier, 2008).

We provide evidence of cytoplasmic stabilization and nuclear accumulation of β-catenin, induced by overexpression of GLI2ΔN in N/TERT human keratinocytes. The loss of membranous β-catenin and its altered localization was also observed after GLI2ΔN expression in 3D organotypic cultures and resembles the expression pattern of β-catenin in human BCCs (El-Bahrawy, El-Masry, 2003, Papanikolaou, Bravou, 2010, Saldanha, Ghura, 2004, Yamazaki, Aragane, 2001, Yang, Andl, 2008), HH/GLI2-driven tumours. Induction of WNTs was also observed in GLI2ΔN-expressing cells suggesting that WNT expression in human BCCs may be regulated by GLI2.

Furthermore, we showed by reporter assay as well as by upregulation of the β-catenin target gene Cyclin-D1 that β-catenin re-localization to the nucleus results in its transcriptional activation, both in stable and inducible GLI2ΔN-expressing cells. Interestingly, the direct upregulation of SOX2 by GLI2ΔN shown here and in other studies (Santini et al. , 2014, Snijders, Huey, 2008, Takanaga et al. , 2009), may further enhance β-catenin-mediated transcriptional activation in GLI2-expressing cells, as SOX2 is a transcription partner for β-catenin, acting in synergy to transcriptionally regulate Cyclin-D1, in breast cancer cells (Chen et al. , 2008). Furthermore, it has been shown that β-catenin is recruited to the promoter of GLI2 in response to TGF-β, which raises the possibility that there may be an amplification loop whereby GLI2 promotes β-catenin

translocation to the nucleus which in turn activates GLI2 transcription (Dennler et al., 2009).

c-MYC, an established target of β-catenin in colon cancer cells (He et al. , 1998, Klaus and Birchmeier, 2008), was downregulated in GLI2-expressing keratinocytes, and has been shown previously to be downregulated in GLI2-expressing rat kidney and HaCaT epithelial cells (Eichberger et al. , 2006, Li et al. , 2007, Regl et al. , 2004a). This pattern is consistent with the reduced expression of c-MYC in human BCCs (Asplund et al. , 2008, Bonifas, Pennypacker, 2001, O'Driscoll, McMorrow, 2006, Regl et al. , 2002).

Activation of WNT/β-catenin pathway by GLI2ΔN suggests that β-catenin can be a downstream effector of SHH/GLI2 pathway and that in human keratinocytes GLI2 is a regulator of β-catenin. In agreement, canonical WNT/β-catenin signaling is essential for the tumorigenic response to deregulated HH signaling, in mice and humans (Roop and Toftgard, 2008, Yang, Andl, 2008).

GLI2 was shown to affect the protein levels of E-cadherin, which is downregulated in many cancers including human BCCs (Papanikolaou, Bravou, 2010) and is a prerequisite for cell transformation, EMT, cancer cell invasion, tumour progression and metastasis (Birchmeier and Behrens, 1994, Canel, Serrels, 2013, Cavallaro and Christofori, 2004, Li, Deng, 2007, Nakajima et al. , 2004). Additionally, high expression of GLI2 together with loss of CDH1 expression is found in melanoma cell lines with a gene expression profile reminiscent of a TGF-b signature that exhibit a strongly invasive phenotype (Hoek

et al. , 2006, Widmer et al. , 2012). In the same context, GLI2 up-regulates and co-operates with ZEB1 to induce CDH1 gene silencing, while GLI2 knock-down restores the levels of CDH1expression (Perrot et al. , 2013). GLI2ΔN-expressing cells also show increased expression of EMT markers SNAIL1 and SNAIL2, which are both transcriptional repressors of the E-cadherin gene (Batlle, Sancho, 2000, Hajra, Chen, 2002). However, in N/TERT epidermal keratinocytes, GLI2ΔN overexpression did not alter the levels of E-cadherin mRNA transcription. It's possible that in N/TERT cells, which retain a normal epithelial differentiation profile, CDH1 expression is tightly regulated and that the reduction of CDH1 protein levels is largely a result of post-translational modification. This is in agreement with other studies where the mechanisms through which SNAIL1 regulates E-cadherin expression are context-specific and in which SNAIL enhances the degradation of E-cadherin protein (Kume et al. , 2013, Stemmer et al. , 2008). Additionally, the upregulation of SNAIL1 upon GLI2ΔN induction could also affect and enhance the transcriptional activity of β-catenin, since SNAIL1 has been shown to bind and act as a co-activator of β-catenin (Stemmer, de Craene, 2008). Moreover, targeted overexpression of SNAIL in mice causes skin cancer including BCC formation, while human BCC show increased expression of SNAIL (De Craene et al. , 2014, Papanikolaou, Bravou, 2010). E-cadherin is the main mediator of cell-cell adhesion and is usually tethered with β-catenin in the epithelial cell membrane. Therefore, its reduced expression upon GLI2ΔN induction, observed both *in vitro* and in organotypic cultures in our study, suggests its possible contribution to the accumulation of β-catenin in the cytoplasm due to release of the membranous β-catenin to the cytoplasm, followed by its subsequent translocation to the nucleus.

E-cadherin cleavage, followed by loosening of AJs and β-catenin redistribution, along with WNT and SNAIL upregulation, which resulted from GLI2 expression, may have implications for both carcinogenesis and invasion. GLI2ΔN keratinocytes invaded organotypic cultures as clusters and multicellular strands, in a manner that recapitulates the histopathology of nodular and superficial human BCC and that is histologically similar to hair buds, for which activation of WNT/β-catenin signaling is required (Yang, Andl, 2008). GLI2 may therefore play a direct role in driving cell invasiveness. Both integrin β1, which mediates focal adhesions, and MMP2 which degrades extracellular matrix (ECM) and is a known target of β-catenin signaling (Wu, Crampton, 2007), were found to be upregulated, especially at the edges of migratory/invasive cells. Both proteins are reported to play major roles in cell migration, invasion and metastasis (Canel, Serrels, 2013, Friedl and Alexander, 2011, Yilmaz and Christofori, 2010). GLI2ΔN overexpressing cells showed diminished invasion capacity in the presence of sFRP-1, with only a minority of the keratinocytes detaching from the epithelium to invade the organotypic ECM. Secreted sFRP-1 proteins act as WNT signaling antagonists, suppressing canonical β-catenin signaling, either by interacting with WNT proteins to prevent them from binding to Frizzled (Fz), or by forming non-functional complexes with Fz (Kawano and Kypta, 2003). This supports the idea that GLI2 promotes the invasive phenotype of human keratinocytes, partly by the up-regulation of secreted WNT proteins, which stimulate canonical WNT/β-catenin signaling. In glioma, a GLI-associated tumour, the infiltrative phenotype is associated with sFRP-1 inhibition and WNT signaling activation (Delic et al. , 2014), while ectopic sFRP-1 reduces glioma cell invasion *in vitro* (Roth et al. , 2000). Furthermore, WNT5A and MMP-2, which we report to be up-

regulated by GLI2 in human keratinocytes, are both linked to the stimulation of glioma cell infiltration (Kamino et al. , 2011).

Finally, we have shown that GLI2 is able to support long-term epidermal regeneration in organotypic cultures. This may be via the maintenance of an undifferentiated basal/stem cell-associated phenotype, resembling that of human BCCs (Crowson, 2006, Miller, 1991, O'Driscoll, McMorrow, 2006, Youssef, Van Keymeulen, 2010). This was associated with down-regulation of keratinocyte differentiation and up-regulation of stem cell markers, including the highly tumorigenic SOX2 embryonic stem cell marker, (Santini, Pietrobono, 2014), and is in line with previous studies (Regl, Kasper, 2004a, Snijders, Huey, 2008). Previously we have shown that GLI2 promotes the survival of genetically unstable keratinocytes by disabling apoptotic mechanisms and deregulating cell cycle proteins such as $p21^{WAF1/CIP1}$ and 14-3-3σ (Pantazi, Gemenetzidis, 2014). Importantly, both proteins have been implicated in the maintenance of epidermal stem cells and are associated with a reduced commitment to differentiation (Dellambra et al. , 2000, Dotto, 2000, Topley et al. , 1999).

Active WNT/β-catenin signaling is known to play an important role in maintaining normal epidermal (Beachy, Karhadkar, 2004, Klaus and Birchmeier, 2008, Nusse et al. , 2008, Reya and Clevers, 2005, Zhu and Watt, 1999) and cancer stem cells (Malanchi et al. , 2008). Moreover, enhanced expression of Snail contributes to the stabilization, expansion and survival of skin stem cells resulting in both skin tumor initiation and malignant progression in mice (De Craene, Denecker, 2014). Therefore, the accumulation

of nuclear β-catenin and its enhanced transactivation, along with the SNAIL upregulation, may act synergistically and contribute to the ability of GLI2ΔN to support long-term epidermal regeneration in organotypic cultures and to induce an undifferentiated basal/stem cell-associated phenotype.

In conclusion, we show that GLI2ΔN is a regulator of β-catenin in human keratinocytes and that its expression supports long-term epidermal regeneration and promotes an invasive undifferentiated basal/stem cell like phenotype with EMT traits. These include the loss of E-cadherin, upregulation of SNAIL, as well as enhanced MMP2 and integrin β1 expression. Altogether, this evidence provide valuable insights into the role of GLI2 in carcinogenesis and tumour progression. Knowledge of the HH/GLI2-WNT/β-catenin crosstalk may also help to identify potential new targets for therapy.

Materials and Methods

Cell lines and culture

Plasmids used to produce cell lines are described in Supplementary Material and Methods. Human telomerase (h/TERT)-immortalised N/TERT-1 (N/TERT) were supplied by Prof. James Rheinwald (Department of Dermatology, Harvard University Medical School, Boston). N/TERT keratinocytes and N/TERT stably expressing EGFP (SINCE) or EGFP-GLI2ΔN (SINEG2) fusion protein were as previously described (Pantazi, Gemenetzidis, 2014), as were Phoenix (human embryonic epithelial 293T derived) cells supplied by Nolan Lab (Medical Center, Stanford University Medical School, CA). NTERT, SINCE and SINEG2 cells were transduced with the pSIN-OT-Luciferase (pSIN-OT-Luc) plasmid, to produce reporter stable (N/TERT-OTLuc, SINCE-OTLuc and SINEG2-OTLuc, respectively) cell lines. Reporter stable cell lines were propagated in RM+ growth medium. Primary human foreskin fibroblasts (HFF) were supplied by Prof. John Marshall (Department of Tumour Biology, Barts Cancer Institute, London) and were cultured as previously described (Shamis et al. , 2011). All cells were grown at 37^{o}C in a humidified atmosphere of 10% (v/v) CO_2/90% (v/v) air. Informed written consent was obtained from all individuals who donated skin biopsies and collaborating dermatologists performed the biopsies at the Royal London Hospital (London, U.K.). The East London and City Health Authority Research Ethics Committee approved the use and protocols for obtaining patient skin biopsies (08/H0704/65).

Retroviral infection

Transductions using pSIN based constructs were carried out as previously described (Pantazi, Gemenetzidis, 2014).

Fluorescent Activated Cell Sorting (FACS)

FACS runs were performed in a BD FACSAria Cell Sorter fitted with a Blue Argon Laser 488nm, violet diode 405nm, and red diode 633nm (BD Biosciences, San Jose, CA) as previously described (Pantazi, Gemenetzidis, 2014).

Light and Fluorescence Microscopy

Cells were visualised using a light fluorescence microscope (Leica DM IRB/Nicon Eclipse TE-2000-S, Leica Microsystems, Germany). Images were captured with a digital imaging system (Leica DC2000 camera).

Reverse Transcription PCR

RNA was extracted from cells using RNeasy Mini Kit (Qiagen, West Sussex, UK) and was reverse transcribed into cDNA with the Reverse transcription kit (Promega, Hampshire, UK) according to manufacturer's protocols.

Real-Time quantitative PCR (qRT-PCR)

qRT-PCR was performed as previously described (Gemenetzidis et al. , 2009, Pantazi, Gemenetzidis, 2014). Samples were analyzed in triplicates and all primer sequences are listed in the Supplementary Data file (Supplementary Table S1).

Subcellular fractionation and Immunoblotting

Cellular fractionation was performed using the Nuclear Extraction Kit (Imgenex, San Diego, CA) according to manufacturer's protocol. Total cell protein extraction and immunoblot analysis was performed as previously described (Gemenetzidis, Bose, 2009, Pantazi, Gemenetzidis, 2014). All primary and secondary antibodies used are listed in Supplementary Data file (Supplementary Table S2).

Luciferase Reporter Assay

The luciferase reporter assay was performed as previously described (Teh et al. , 2007) and as described in Supplementary Material and Methods.

Organotypic Cultures

Three dimensional (3D) organotypic keratinocyte cultures on collagen gels were constructed, cultured, processed, sectioned, H&E-stained and imaged as previously described (Nystrom et al. , 2005) and as described in Supplementary Material and Methods. For the treatment with sFRP-1 (recombinant human sFRP-1 protein, CF; R&D Systems, UK), organotypic cultures were incubated with growth medium supplemented with 0.1 μg/ml sFRP-1 and medium was replaced every second day. Control gels were incubated with growth medium supplemented with vehicle (PBS 0.1%BSA).

Immunofluorescence and confocal microscopy

Cytokeratin was immunostained with a mouse monoclonal antibody (anti-human cytokeratin antibody AE1/AE3 (DakoCytomation) at 1:200 dilution, on 4μm paraffin sections as described in Supplementary Materials and Methods. Images were acquired

with a Zeiss LSM 710 Meta confocal microscope (Carl Zeiss Jena, Carl Zeiss Ltd, UK), using the Zen image processing and analysis software.

Quantification of cell invasion

Consecutive digital and fluorescence images of DAPI and cytokeratin stained sections were captured using a fluorescence confocal microscope (Zeiss LSM 710 Meta) across the whole length of the gel. Images were imported into ImageJ and cells were counted using the cell counter function. Cytokeratin and DAPI positive cells present below the basement membrane, were counted as invading cells, and a total count of invading cells per gel was derived. 8 (14-day) and 7 (28-day) collagen gels were counted for each cell line.

Immunohistochemistry

Immunohistochemistry was performed using an E-cadherin mouse monoclonal antibody (Flex, IS059, Ready to use, DakoCytomation), β-catenin mouse monoclonal antibody (Flex, IS702, Ready to use, DakoCytomation), MMP2 rabbit polyclonal antibody (ab37150, 1:100, Abcam) as described in Supplementary Material and Methods. Staining was imaged on the NanoZoomer Digital Pathology (NDP) whole slide scanner (Hamamatsu) in brightfield mode, using the Viewing Software NDP.view2 U12388-01 image processing and analysis software.

Statistical analysis

Statistical analysis was performed using Microsoft Excel's software, GraphPad's InStat (V2-04a) and Prism Software (V5,0) (Graph-Pad Software, San Diego, CA) for student's *t* test analysis.

Conflict of interest

The authors state no conflict of interest.

Acknowledgements

We thank Prof. James Rheinwald (Department of Dermatology, Harvard University Medical School, Boston) for providing the N/TERT-1 (N/TERT) cell line. We are grateful to Dr Paul Khavari (Stanford University School of Medicine, CA) for providing the retroviral pSIN-CMV-EGFP plasmid, Prof. Fritz Aberger (Department of Molecular Biology, University of Salzburg, Austria) for providing the pCMV-EGFP-GLI2ΔN plasmid and Prof. Bert Vogelstein (The John Hopkins Oncology Centre Baltimore, MD) for providing the Tcf-4 responsive luciferase plasmid pGL3-OT (OT-β-catenin responsive promoter), an improved version of TOPFLASH. We also thank Prof. John Marshall (Department of Tumour Biology, Barts Cancer Institute, London) for providing the human foreskin fibroblast (HFF) cell line. We also thank Prof. Kenneth E. Parkinson for his constructive comments. This work was supported by funding from St Bartholmew's and the Royal London Charitable Foundation.

References

Aberger F, Ruiz IAA. Context-dependent signal integration by the GLI code: the oncogenic load, pathways, modifiers and implications for cancer therapy. Seminars in cell & developmental biology. 2014;33:93-104.

Alexaki VI, Javelaud D, Van Kempen LC, Mohammad KS, Dennler S, Luciani F, et al. GLI2-mediated melanoma invasion and metastasis. Journal of the National Cancer Institute. 2010;102:1148-59.

Asplund A, Gry Bjorklund M, Sundquist C, Stromberg S, Edlund K, Ostman A, et al. Expression profiling of microdissected cell populations selected from basal cells in normal epidermis and basal cell carcinoma. The British journal of dermatology. 2008;158:527-38.

Batlle E, Sancho E, Franci C, Dominguez D, Monfar M, Baulida J, et al. The transcription factor snail is a repressor of E-cadherin gene expression in epithelial tumour cells. Nature cell biology. 2000;2:84-9.

Beachy PA, Karhadkar SS, Berman DM. Tissue repair and stem cell renewal in carcinogenesis. Nature. 2004;432:324-31.

Behrens J, von Kries JP, Kuhl M, Bruhn L, Wedlich D, Grosschedl R, et al. Functional interaction of beta-catenin with the transcription factor LEF-1. Nature. 1996;382:638-42.

Birchmeier W, Behrens J. Cadherin expression in carcinomas: role in the formation of cell junctions and the prevention of invasiveness. Biochimica et biophysica acta. 1994;1198:11-26.

Bonifas JM, Pennypacker S, Chuang PT, McMahon AP, Williams M, Rosenthal A, et al. Activation of expression of hedgehog target genes in basal cell carcinomas. The Journal of investigative dermatology. 2001;116:739-42.

Brabletz T, Hlubek F, Spaderna S, Schmalhofer O, Hiendlmeyer E, Jung A, et al. Invasion and metastasis in colorectal cancer: epithelial-mesenchymal transition, mesenchymal-epithelial transition, stem cells and beta-catenin. Cells, tissues, organs. 2005;179:56-65.

Canel M, Serrels A, Frame MC, Brunton VG. E-cadherin-integrin crosstalk in cancer invasion and metastasis. Journal of cell science. 2013;126:393-401.

Cavallaro U, Christofori G. Cell adhesion and signaling by cadherins and Ig-CAMs in cancer. Nature reviews. 2004;4:118-32.

Chang YW, Jakobi R, McGinty A, Foschi M, Dunn MJ, Sorokin A. Cyclooxygenase 2 promotes cell survival by stimulation of dynein light chain expression and inhibition of neuronal nitric oxide synthase activity. Molecular and cellular biology. 2000;20:8571-9.

Chen Y, Shi L, Zhang L, Li R, Liang J, Yu W, et al. The molecular mechanism governing the oncogenic potential of SOX2 in breast cancer. The Journal of biological chemistry. 2008;283:17969-78.

Chi TY, Chen GG, Ho LK, Lai PB. Establishment of a doxycycline-regulated cell line with inducible, doubly-stable expression of the wild-type p53 gene from p53-deleted hepatocellular carcinoma cells. Cancer cell international. 2005;5:27.

Crowson AN. Basal cell carcinoma: biology, morphology and clinical implications. Mod Pathol. 2006;19 Suppl 2:S127-47.

Daya-Grosjean L, Couve-Privat S. Sonic hedgehog signaling in basal cell carcinomas. Cancer letters. 2005;225:181-92.

De Craene B, Denecker G, Vermassen P, Taminau J, Mauch C, Derore A, et al. Epidermal Snail expression drives skin cancer initiation and progression through enhanced cytoprotection, epidermal stem/progenitor cell expansion and enhanced metastatic potential. Cell death and differentiation. 2014;21:310-20.

Delic S, Lottmann N, Stelzl A, Liesenberg F, Wolter M, Gotze S, et al. MiR-328 promotes glioma cell invasion via SFRP1-dependent Wnt-signaling activation. Neuro-oncology. 2014;16:179-90.

Dellambra E, Golisano O, Bondanza S, Siviero E, Lacal P, Molinari M, et al. Downregulation of 14-3-3sigma prevents clonal evolution and leads to immortalization of primary human keratinocytes. The Journal of cell biology. 2000;149:1117-30.

Deng H, Lin Q, Khavari PA. Sustainable cutaneous gene delivery. Nature biotechnology. 1997;15:1388-91.

Dennler S1, André J, Verrecchia F, Mauviel A. Cloning of the human GLI2 Promoter: transcriptional activation by transforming growth factor-beta via SMAD3/beta-catenin cooperation. Journal of Biological Chemistry. 2009;284(46):31523-31.

Dotto GP. p21(WAF1/Cip1): more than a break to the cell cycle? Biochimica et biophysica acta. 2000;1471:M43-56.

Eichberger T, Sander V, Schnidar H, Regl G, Kasper M, Schmid C, et al. Overlapping and distinct transcriptional regulator properties of the GLI1 and GLI2 oncogenes. Genomics. 2006;87:616-32.

El-Bahrawy M, El-Masry N, Alison M, Poulsom R, Fallowfield M. Expression of beta-catenin in basal cell carcinoma. The British journal of dermatology. 2003;148:964-70.

Fong H, Hohenstein KA, Donovan PJ. Regulation of self-renewal and pluripotency by Sox2 in human embryonic stem cells. Stem cells (Dayton, Ohio). 2008;26:1931-8.

Friedl P, Alexander S. Cancer invasion and the microenvironment: plasticity and reciprocity. Cell. 2011;147:992-1009.

Gandarillas A, Watt FM. c-MYC promotes differentiation of human epidermal stem cells. Genes & development. 1997;11:2869-82.

Gat U, DasGupta R, Degenstein L, Fuchs E. De Novo hair follicle morphogenesis and hair tumors in mice expressing a truncated beta-catenin in skin. Cell. 1998;95:605-14.

Gemenetzidis E, Bose A, Riaz AM, Chaplin T, Young BD, Ali M, et al. FOXM1 upregulation is an early event in human squamous cell carcinoma and it is enhanced by nicotine during malignant transformation. PLoS ONE. 2009;4:e4849.

Gorlin RJ. Nevoid basal cell carcinoma syndrome. Dermatologic clinics. 1995;13:113-25.

Grachtchouk M, Mo R, Yu S, Zhang X, Sasaki H, Hui CC, et al. Basal cell carcinomas in mice overexpressing Gli2 in skin. Nature genetics. 2000;24:216-7.

Hajra KM, Chen DY, Fearon ER. The SLUG zinc-finger protein represses E-cadherin in breast cancer. Cancer research. 2002;62:1613-8.

He TC, Sparks AB, Rago C, Hermeking H, Zawel L, da Costa LT, et al. Identification of c-MYC as a target of the APC pathway. Science (New York, NY. 1998;281:1509-12.

Hoek KS, Schlegel NC, Brafford P, Sucker A, Ugurel S, Kumar R, et al. Metastatic potential of melanomas defined by specific gene expression profiles with no BRAF signature. Pigment cell research / sponsored by the European Society for Pigment Cell Research and the International Pigment Cell Society. 2006;19:290-302.

Huelsken J, Vogel R, Erdmann B, Cotsarelis G, Birchmeier W. beta-Catenin controls hair follicle morphogenesis and stem cell differentiation in the skin. Cell. 2001;105:533-45.

Hugo H, Ackland ML, Blick T, Lawrence MG, Clements JA, Williams ED, et al. Epithelial--mesenchymal and mesenchymal--epithelial transitions in carcinoma progression. Journal of cellular physiology. 2007;213:374-83.

Hutchin ME, Kariapper MS, Grachtchouk M, Wang A, Wei L, Cummings D, et al. Sustained Hedgehog signaling is required for basal cell carcinoma proliferation and survival: conditional skin tumorigenesis recapitulates the hair growth cycle. Genes & development. 2005;19:214-23.

Ikram MS, Neill GW, Regl G, Eichberger T, Frischauf AM, Aberger F, et al. GLI2 is expressed in normal human epidermis and BCC and induces GLI1 expression by binding to its promoter. The Journal of investigative dermatology. 2004;122:1503-9.

Javelaud D, Alexaki VI, Dennler S, Mohammad KS, Guise TA, Mauviel A. TGF-beta/SMAD/GLI2 signaling axis in cancer progression and metastasis. Cancer research. 2011;71:5606-10.

Jones PH, Harper S, Watt FM. Stem cell patterning and fate in human epidermis. Cell. 1995;80:83-93.

Jones PH, Watt FM. Separation of human epidermal stem cells from transit amplifying cells on the basis of differences in integrin function and expression. Cell. 1993;73:713-24.

Kamino M, Kishida M, Kibe T, Ikoma K, Iijima M, Hirano H, et al. Wnt-5a signaling is correlated with infiltrative activity in human glioma by inducing cellular migration and MMP-2. Cancer science. 2011;102:540-8.

Kawano Y, Kypta R. Secreted antagonists of the Wnt signaling pathway. Journal of cell science. 2003;116:2627-34.

Kim K, Lu Z, Hay ED. Direct evidence for a role of beta-catenin/LEF-1 signaling pathway in induction of EMT. Cell biology international. 2002;26:463-76.

Klaus A, Birchmeier W. Wnt signaling and its impact on development and cancer. Nature reviews. 2008;8:387-98.

Korinek V, Barker N, Morin PJ, van Wichen D, de Weger R, Kinzler KW, et al. Constitutive transcriptional activation by a beta-catenin-Tcf complex in APC-/- colon carcinoma. Science (New York, NY. 1997;275:1784-7.

Kume K, Haraguchi M, Hijioka H, Ishida T, Miyawaki A, Nakamura N, et al. The transcription factor Snail enhanced the degradation of E-cadherin and desmoglein 2 in oral squamous cell carcinoma cells. Biochemical and biophysical research communications. 2013;430:889-94.

Li X, Deng W, Lobo-Ruppert SM, Ruppert JM. Gli1 acts through Snail and E-cadherin to promote nuclear signaling by beta-catenin. Oncogene. 2007;26:4489-98.

Li ZJ, Mack SC, Mak TH, Angers S, Taylor MD, Hui CC. Evasion of p53 and G2/M checkpoints are characteristic of Hh-driven basal cell carcinoma. Oncogene. 2014;33:2674-80.

Malanchi I, Peinado H, Kassen D, Hussenet T, Metzger D, Chambon P, et al. Cutaneous cancer stem cell maintenance is dependent on beta-catenin signaling. Nature. 2008;452:650-3.

Marchenko GN, Marchenko ND, Leng J, Strongin AY. Promoter characterization of the novel human matrix metalloproteinase-26 gene: regulation by the T-cell factor-4 implies specific expression of the gene in cancer cells of epithelial origin. The Biochemical journal. 2002;363:253-62.

Marsh D, Dickinson S, Neill GW, Marshall JF, Hart IR, Thomas GJ. alpha vbeta 6 Integrin promotes the invasion of morphoeic basal cell carcinoma through stromal modulation. Cancer research. 2008;68:3295-303.

Masui S, Nakatake Y, Toyooka Y, Shimosato D, Yagi R, Takahashi K, et al. Pluripotency governed by Sox2 via regulation of Oct3/4 expression in mouse embryonic stem cells. Nature cell biology. 2007;9:625-35.

Miller AD, Chen F. Retrovirus packaging cells based on 10A1 murine leukemia virus for production of vectors that use multiple receptors for cell entry. Journal of virology. 1996;70:5564-71.

Miller SJ. Biology of basal cell carcinoma (Part I). Journal of the American Academy of Dermatology. 1991;24:1-13.

Muffler S, Stark HJ, Amoros M, Falkowska-Hansen B, Boehnke K, Buhring HJ, et al. A stable niche supports long-term maintenance of human epidermal stem cells in organotypic cultures. Stem cells (Dayton, Ohio). 2008;26:2506-15.

Mullor JL, Dahmane N, Sun T, Ruiz i Altaba A. Wnt signals are targets and mediators of Gli function. Curr Biol. 2001;11:769-73.

Nakajima S, Doi R, Toyoda E, Tsuji S, Wada M, Koizumi M, et al. N-cadherin expression and epithelial-mesenchymal transition in pancreatic carcinoma. Clinical cancer research : an official journal of the American Association for Cancer Research. 2004;10:4125-33.

Nelson WJ, Nusse R. Convergence of Wnt, beta-catenin, and cadherin pathways. Science (New York, NY. 2004;303:1483-7.

Nicolas M, Wolfer A, Raj K, Kummer JA, Mill P, van Noort M, et al. Notch1 functions as a tumor suppressor in mouse skin. Nature genetics. 2003;33:416-21.

Niwa H. How is pluripotency determined and maintained? Development (Cambridge, England). 2007;134:635-46.

Nusse R, Fuerer C, Ching W, Harnish K, Logan C, Zeng A, et al. Wnt signaling and stem cell control. Cold Spring Harbor symposia on quantitative biology. 2008;73:59-66.

Nystrom ML, Thomas GJ, Stone M, Mackenzie IC, Hart IR, Marshall JF. Development of a quantitative method to analyse tumour cell invasion in organotypic culture. The Journal of pathology. 2005;205:468-75.

O'Driscoll L, McMorrow J, Doolan P, McKiernan E, Mehta JP, Ryan E, et al. Investigation of the molecular profile of basal cell carcinoma using whole genome microarrays. Molecular cancer. 2006;5:74.

Pantazi E, Gemenetzidis E, Trigiante G, Warnes G, Shan L, Mao X, et al. GLI2 induces genomic instability in human keratinocytes by inhibiting apoptosis. Cell death & disease. 2014;5:e1028.

Papanikolaou S, Bravou V, Gyftopoulos K, Nakas D, Repanti M, Papadaki H. ILK expression in human basal cell carcinoma correlates with epithelial-mesenchymal transition markers and tumour invasion. Histopathology. 2010;56:799-809.

Perrot CY, Gilbert C, Marsaud V, Postigo A, Javelaud D, Mauviel A. GLI2 cooperates with ZEB1 for transcriptional repression of CDH1 expression in human melanoma cells. Pigment cell & melanoma research. 2013;26:861-73.

Polakis P. Wnt signaling and cancer. Genes & development. 2000;14:1837-51.

Regl G, Kasper M, Schnidar H, Eichberger T, Neill GW, Ikram MS, et al. The zinc-finger transcription factor GLI2 antagonizes contact inhibition and differentiation of human epidermal cells. Oncogene. 2004a;23:1263-74.

Regl G, Kasper M, Schnidar H, Eichberger T, Neill GW, Philpott MP, et al. Activation of the BCL2 promoter in response to Hedgehog/GLI signal transduction is predominantly mediated by GLI2. Cancer research. 2004b;64:7724-31.

Regl G, Neill GW, Eichberger T, Kasper M, Ikram MS, Koller J, et al. Human GLI2 and GLI1 are part of a positive feedback mechanism in Basal Cell Carcinoma. Oncogene. 2002;21:5529-39.

Reya T, Clevers H. Wnt signaling in stem cells and cancer. Nature. 2005;434:843-50.

Roop D, Toftgard R. Hedgehog in wnterland. Nature genetics. 2008;40:1040-1.

Roth W, Wild-Bode C, Platten M, Grimmel C, Melkonyan HS, Dichgans J, et al. Secreted Frizzled-related proteins inhibit motility and promote growth of human malignant glioma cells. Oncogene. 2000;19:4210-20.

Ruiz i Altaba A, Sanchez P, Dahmane N. Gli and hedgehog in cancer: tumours, embryos and stem cells. Nature reviews. 2002;2:361-72.

Saldanha G, Ghura V, Potter L, Fletcher A. Nuclear beta-catenin in basal cell carcinoma correlates with increased proliferation. The British journal of dermatology. 2004;151:157-64.

Santini R, Pietrobono S, Pandolfi S, Montagnani V, D'Amico M, Penachioni JY, et al. SOX2 regulates self-renewal and tumorigenicity of human melanoma-initiating cells. Oncogene. 2014;33:4697-708.

Shamis Y, Hewitt KJ, Carlson MW, Margvelashvilli M, Dong S, Kuo CK, et al. Fibroblasts derived from human embryonic stem cells direct development and repair of 3D human skin equivalents. Stem cell research & therapy. 2011;2:10.

Shih IM, Yu J, He TC, Vogelstein B, Kinzler KW. The beta-catenin binding domain of adenomatous polyposis coli is sufficient for tumor suppression. Cancer research. 2000;60:1671-6.

Shtutman M, Zhurinsky J, Simcha I, Albanese C, D'Amico M, Pestell R, et al. The cyclin D1 gene is a target of the beta-catenin/LEF-1 pathway. Proceedings of the National Academy of Sciences of the United States of America. 1999;96:5522-7.

Snijders AM, Huey B, Connelly ST, Roy R, Jordan RC, Schmidt BL, et al. Stromal control of oncogenic traits expressed in response to the overexpression of GLI2, a pleiotropic oncogene. Oncogene. 2008.

Stark HJ, Baur M, Breitkreutz D, Mirancea N, Fusenig NE. Organotypic keratinocyte cocultures in defined medium with regular epidermal morphogenesis and differentiation. The Journal of investigative dermatology. 1999;112:681-91.

Stemmer V, de Craene B, Berx G, Behrens J. Snail promotes Wnt target gene expression and interacts with beta-catenin. Oncogene. 2008;27:5075-80.

Sterling JA, Oyajobi BO, Grubbs B, Padalecki SS, Munoz SA, Gupta A, et al. The hedgehog signaling molecule Gli2 induces parathyroid hormone-related peptide expression and osteolysis in metastatic human breast cancer cells. Cancer research. 2006;66:7548-53.

Sternlicht MD, Lochter A, Sympson CJ, Huey B, Rougier JP, Gray JW, et al. The stromal proteinase MMP3/stromelysin-1 promotes mammary carcinogenesis. Cell. 1999;98:137-46.

Takanaga H, Tsuchida-Straeten N, Nishide K, Watanabe A, Aburatani H, Kondo T. Gli2 is a novel regulator of sox2 expression in telencephalic neuroepithelial cells. Stem cells (Dayton, Ohio). 2009;27:165-74.

Teh MT, Blaydon D, Ghali LR, Briggs V, Edmunds S, Pantazi E, et al. Role for WNT16B in human epidermal keratinocyte proliferation and differentiation. Journal of cell science. 2007;120:330-9.

Tetsu O, McCormick F. Beta-catenin regulates expression of cyclin D1 in colon carcinoma cells. Nature. 1999;398:422-6.

Thiery JP. Epithelial-mesenchymal transitions in tumour progression. Nature reviews. 2002;2:442-54.

Thiyagarajan S, Bhatia N, Reagan-Shaw S, Cozma D, Thomas-Tikhonenko A, Ahmad N, et al. Role of GLI2 transcription factor in growth and tumorigenicity of prostate cells. Cancer research. 2007;67:10642-6.

Tojo M, Kiyosawa H, Iwatsuki K, Nakamura K, Kaneko F. Expression of the GLI2 oncogene and its isoforms in human basal cell carcinoma. The British journal of dermatology. 2003;148:892-7.

Topley GI, Okuyama R, Gonzales JG, Conti C, Dotto GP. p21(WAF1/Cip1) functions as a suppressor of malignant skin tumor formation and a determinant of keratinocyte stem-cell potential. Proceedings of the National Academy of Sciences of the United States of America. 1999;96:9089-94.

Widmer DS, Cheng PF, Eichhoff OM, Belloni BC, Zipser MC, Schlegel NC, et al. Systematic classification of melanoma cells by phenotype-specific gene expression mapping. Pigment cell & melanoma research. 2012;25:343-53.

Wu B, Crampton SP, Hughes CC. Wnt signaling induces matrix metalloproteinase expression and regulates T cell transmigration. Immunity. 2007;26:227-39.

Yamazaki F, Aragane Y, Kawada A, Tezuka T. Immunohistochemical detection for nuclear beta-catenin in sporadic basal cell carcinoma. The British journal of dermatology. 2001;145:771-7.

Yang SH, Andl T, Grachtchouk V, Wang A, Liu J, Syu LJ, et al. Pathological responses to oncogenic Hedgehog signaling in skin are dependent on canonical Wnt/beta3-catenin signaling. Nature genetics. 2008;40:1130-5.

Yilmaz M, Christofori G. Mechanisms of motility in metastasizing cells. Molecular cancer research : MCR. 2010;8:629-42.

Yin WC, Li ZJ, Hui CC. BCC or not: Sufu keeps it in check. Oncoscience. 2015;2:77-8.

Youssef KK, Van Keymeulen A, Lapouge G, Beck B, Michaux C, Achouri Y, et al. Identification of the cell lineage at the origin of basal cell carcinoma. Nature cell biology. 2010;12:299-305.

Yu M, Zloty D, Cowan B, Shapiro J, Haegert A, Bell RH, et al. Superficial, nodular, and morpheiform basal-cell carcinomas exhibit distinct gene expression profiles. The Journal of investigative dermatology. 2008;128:1797-805.

Zhang D, Cao L, Li Y, Lu H, Yang X, Xue P. Expression of glioma-associated oncogene 2 (Gli 2) is correlated with poor prognosis in patients with hepatocellular carcinoma undergoing hepatectomy. World journal of surgical oncology. 2013;11:25.

Zhu AJ, Haase I, Watt FM. Signaling via beta1 integrins and mitogen-activated protein kinase determines human epidermal stem cell fate in vitro. Proceedings of the National Academy of Sciences of the United States of America. 1999;96:6728-33.

Zhu AJ, Watt FM. beta-catenin signaling modulates proliferative potential of human epidermal keratinocytes independently of intercellular adhesion. Development (Cambridge, England). 1999;126:2285-98.

Figure Legends

Figure 1. GLI2ΔN induces nuclear re-localization of β-catenin and promotes its transcriptional activity. Immunoblotting for β-catenin, after cytoplasmic and nuclear protein fractionation on SINCE **(a)** and SINEG2 **(b)** cell lines, and on whole protein extracts **(c)**. Lamin-B1 and GAPDH were used as nuclear and cytoplasmic markers, respectively, and β-actin was used as loading control. **(d)** Immunoblot densitometry analysis reveals a nearly 10-fold increase in the ratio of nuclear:cytoplasmic protein levels of β-catenin in SINEG2 cells, compared to SINCE cells. ** *P≤0.01* **(e)** Luciferase reporter assay on N/TERT, SINCE and SINEG2 cells. OT-β-catenin responsive promoter was significantly induced in SINEG2 cells, compared to SINCE and N/TERT controls. Each bar represents a mean ± s.e.m of normalised to protein content triplicate samples. ** *P≤0.01*.

Figure 2: GLI2ΔN expression in N/TERT keratinocytes induces WNT genes expression. RNA was harvested from N/TERT, SINCE, and SINEG2 cells to examine the levels of WNT5A **(a)**, WNT7A **(b)**, and WNT11 **(c)** mRNA expression using primers specific for each gene. Quantitative RT-PCR analysis of WNT5A, WNT7A and WNT11 showed an increase in expression of all the three genes in SINEG2 cells compared to N/TERT and SINCE control cells. Each bar represents mean fold induction relative to N/TERT (arbitrary value of 1) ± s.e.m of triplicate samples. *** *P≤0.001*.

Figure 3: Protein downregulation of E-cadherin and mRNA upregulation of SNAIL1 and SNAIL2 in GLI2ΔN-expressing keratinocytes. (a) SINEG2 cells show a marked decrease of E-cadherin protein levels compared to N/TERT and SINCE control cells. B-actin was used as a protein loading control. RNA was harvested from N/TERT, SINCE, and SINEG2 cells to examine the levels of SNAIL1 **(b)**, SNAIL2 **(c)**, and E-cadherin **(c)** mRNA expression using primers specific for each gene. Quantitative RT-PCR analysis of SNAIL1, SNAIL2 and E-cadherin showed an increase in expression of both SNAIL genes in SINEG2 cells compared to N/TERT and SINCE control cells, but no difference in expression of E-cadherin gene. Each bar represents mean fold induction relative to N/TERT (arbitrary value of 1) ± s.e.m of triplicate samples. ** $P \leq 0.01$.

Figure 4: Invasion of collagen/matrigel gels by GLI2ΔN-expressing cells. 14-day organotypic cultures of N/TERT, SINCE and SINEG2 cells, stained with **(a)** H&E staining **(b)** cytokeratin (red) and DAPI (blue), showing invasion of SINEG2 keratinocytes. N/TERT and SINCE produced a stratified epithelium, whereas, SINEG2 collectively invade into the gel. Scale bar: **(a)** 100µm, **(b)** 50µm. **(c)** Quantification of the total invading cell numbers at 14 days shows a significant increase of invading SINEG2 cell numbers compared to control N/TERT and SINCE cells. Each data point represents the total number of invading cells per gel (n=8 from three independent experiments). Each bar represents the median with interquartile range of all data points. ** $P \leq 0.01$.

Figure 5: E-cadherin and β-catenin expression in 3D-organotypic cultures. Staining for **(a)** E-cadherin and **(b)** β-catenin in 14-day organotypic cultures of SINCE and SINEG2 cells. Expression of E-cadherin in SINCE cells (top panel) shows strong continuous membranous staining, compared to weaker expression in SINEG2 cell (lower two panels)**,** showing loss or fragmentation of membranous E-cadherin staining. **(b)** Expression of β-catenin in SINCE cells (top panel) shows continuous membranous staining, compared to SINEG2 cells (lower two panels) showing loss or partial loss of membranous β-catenin staining with altered cellular distribution in the cytoplasm and **(c)** focally in the nucleus (black arrow). Scale bar: **(a, b)** 100µm, **(c)** 10µm.

Figure 6: GLI2ΔN induces extended epidermal regeneration, in long-term organotypic cultures and an undifferentiated stem-cell like gene expression profile *in vitro*. 28-day organotypic cultures stained with **(a)** H&E, **(b)** cytokeratin (red) and DAPI (blue), shows epidermal atrophy of N/TERT and SINCE cells,, while SINEG cells display a stratified epithelium with collective keratinocyte invasion. **(c)** Deep single-cell invasion (white arrow) and multicellular solid strand invasion (yellow arrow) was also observed in 28-day collagen gels (SINEG2). Scale bar: **(a)** 100µm, **(b)** 50µm, **(c, e)** 100µm. A significant increase in invading SINEG2 cells compared to N/TERT and SINCE cells is shown in **(d)**. Each data point represents the total number of invading cells per gel (n=7) from two independent experiments. Each bar represents the median with interquartile range of all data points. ** $P \leq 0.01$. Involucrin **(f)**, c-MYC **(g),** Integrin β1 **(h)** and SOX2 **(i)** expression in SINEG2 cells. Each bar represents mean fold suppression/or induction relative to N/TERT (arbitrary value of 1) ± s.e.m of triplicate

samples. * *P≤0.05*, *** *P≤0.001*. **(j)** C-MYC protein levels were reduced in SINEG2 cells. B-actin was used as loading control.

Figure 1

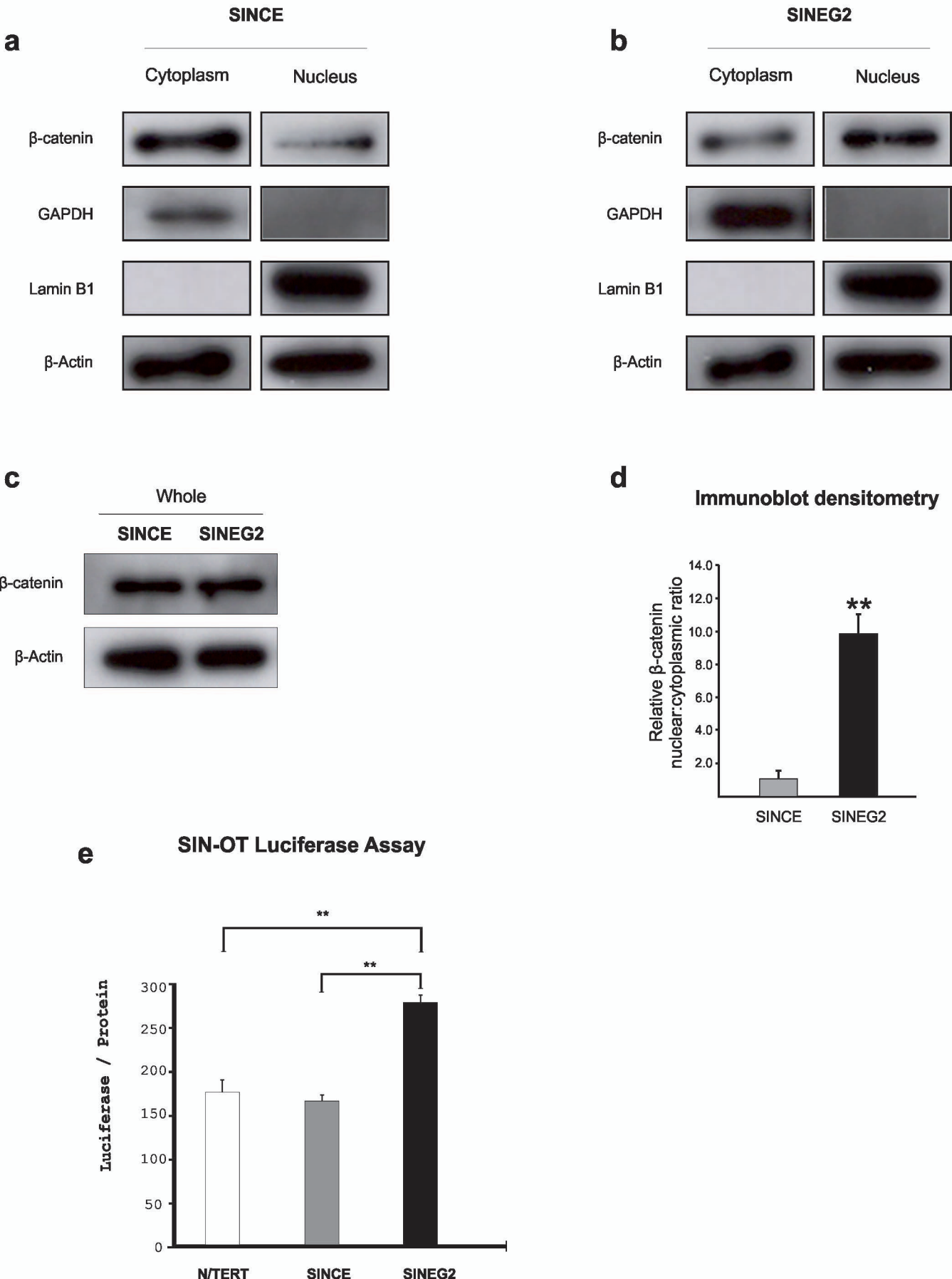
a
SINCE
Cytoplasm
Nucleus
β-catenin
GAPDH
Lamin B1
β-Actin
b
SINEG2
Cytoplasm
Nucleus
β-catenin
GAPDH
Lamin B1
β-Actin
c
Whole
SINCE
SINEG2
β-catenin
β-Actin
d
Immunoblot densitometry
Relative β-catenin nuclear:cytoplasmic ratio
14.0
12.0
10.0
8.0
6.0
4.0
2.0
**
SINCE
SINEG2
e
SIN-OT Luciferase Assay
Luciferase / Protein
300
250
200
150
100
50
0
**
**
N/TERT
SINCE
SINEG2

Figure 2

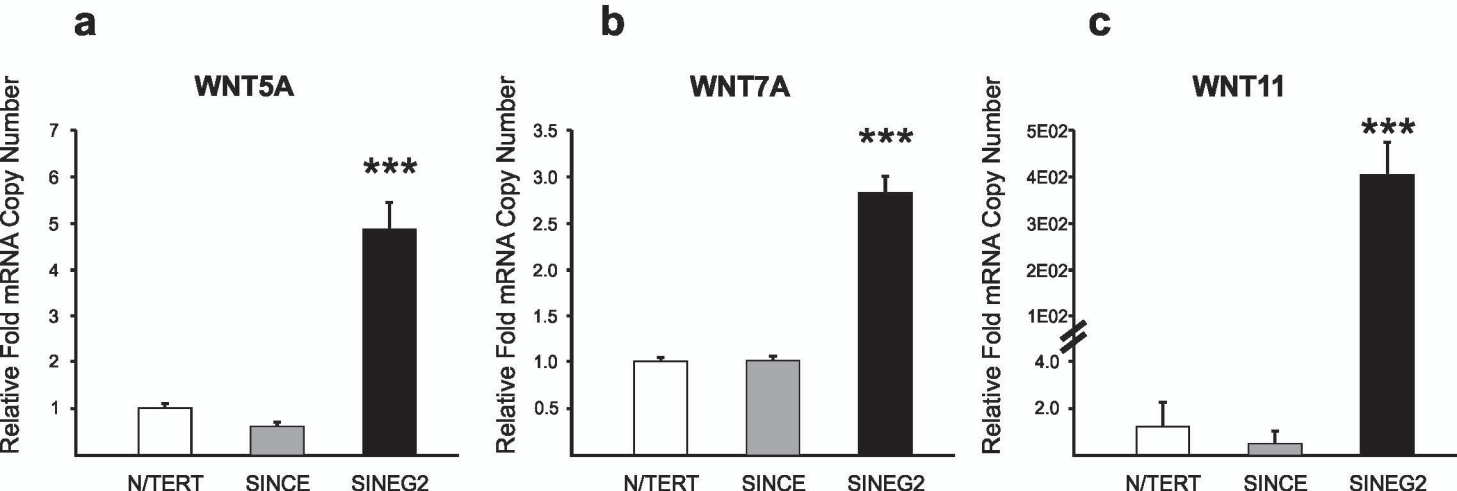
a
WNT5A
Relative Fold mRNA Copy Number
7
6
5
4
3
2
1
***
N/TERT
SINCE
SINEG2
b
WNT7A
Relative Fold mRNA Copy Number
3.5
3.0
2.5
2.0
1.5
1.0
0.5
***
N/TERT
SINCE
SINEG2
c
WNT11
Relative Fold mRNA Copy Number
5E02
4E02
3E02
2E02
1E02
4.0
2.0
***
N/TERT
SINCE
SINEG2

Figure 3

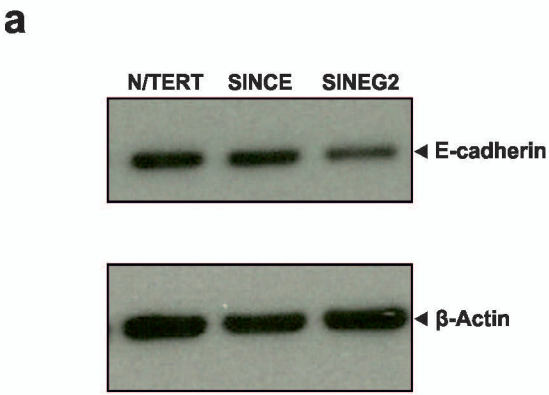
a
N/TERT
SINCE
SINEG2
E-cadherin
β-Actin

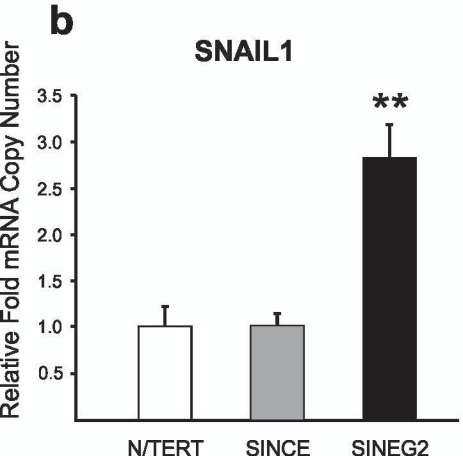
b
SNAIL1
Relative Fold mRNA Copy Number
3.5
3.0
2.5
2.0
1.5
1.0
0.5
**
N/TERT
SINCE
SINEG2

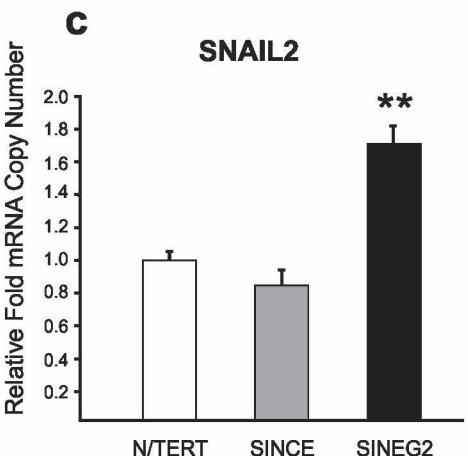
c
SNAIL2
Relative Fold mRNA Copy Number
2.0
1.8
1.6
1.4
1.2
1.0
0.8
0.6
0.4
0.2
**
N/TERT
SINCE
SINEG2

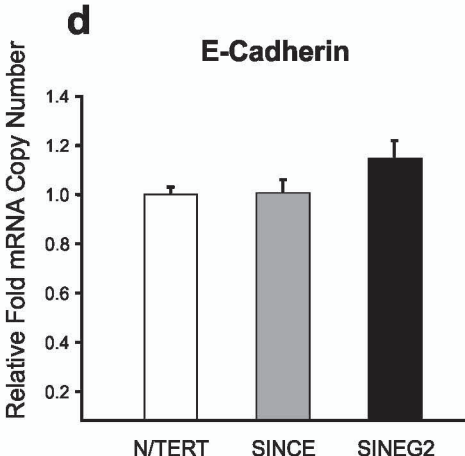
d
E-Cadherin
Relative Fold mRNA Copy Number
1.4
1.2
1.0
0.8
0.6
0.4
0.2
N/TERT
SINCE
SINEG2

Figure 4

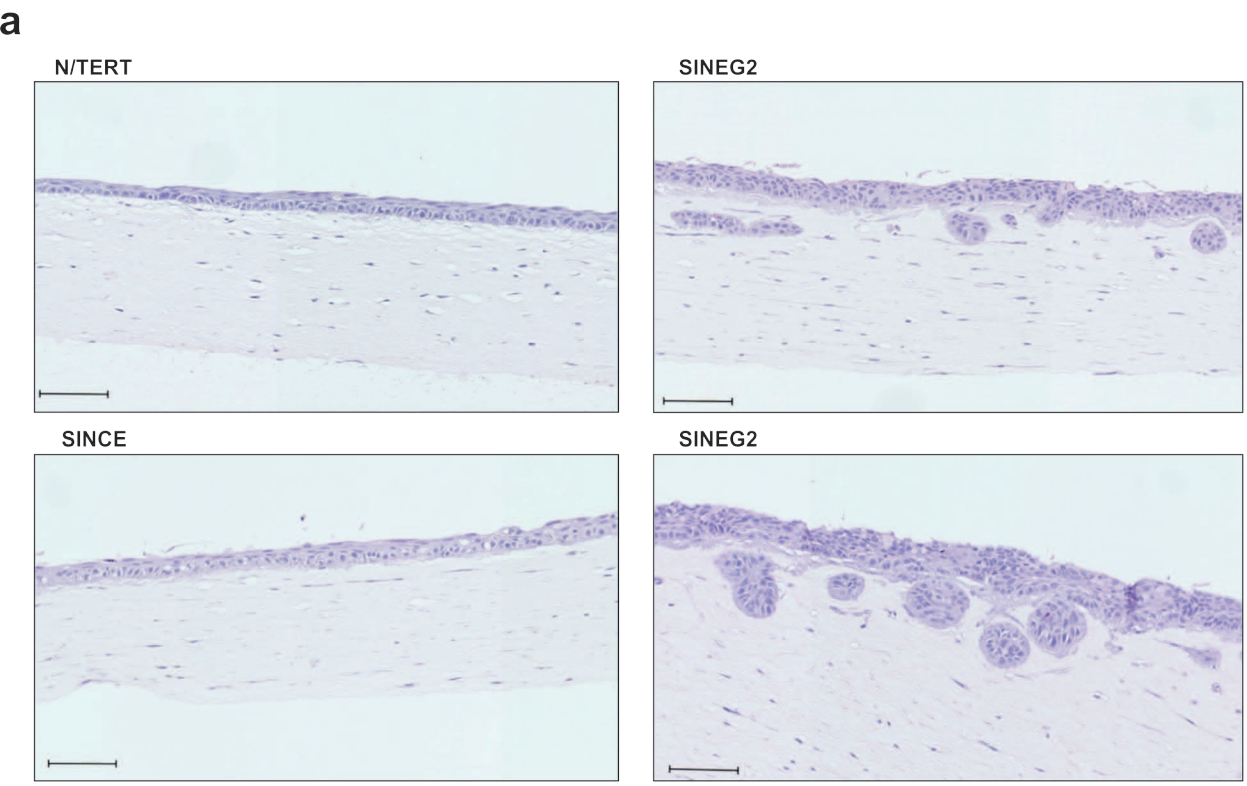
a
N/TERT
SINEG2
SINCE
SINEG2

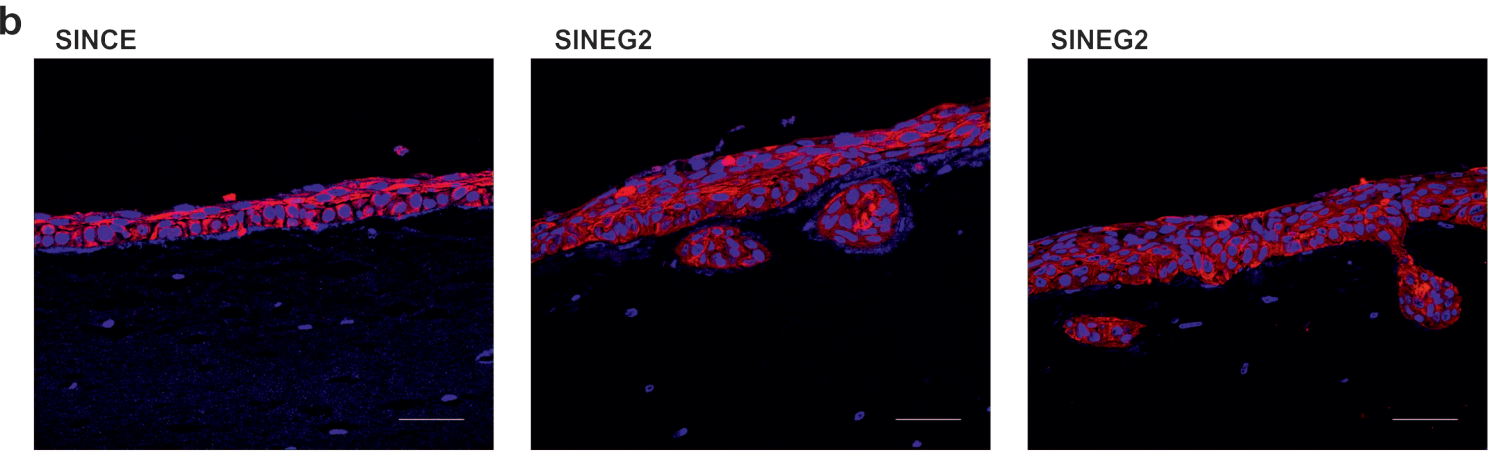
b
SINCE
SINEG2
SINEG2

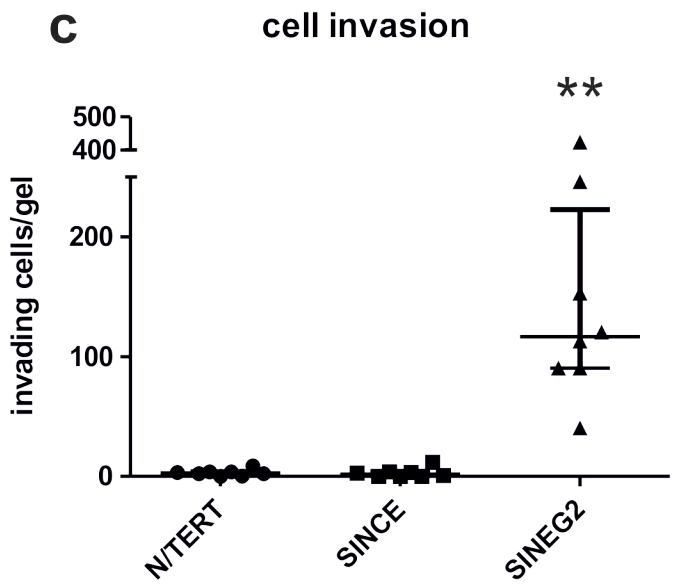
c
cell invasion
**
500
400
200
100
0
invading cells/gel
N/TERT
SINCE
SINEG2

Figure 5

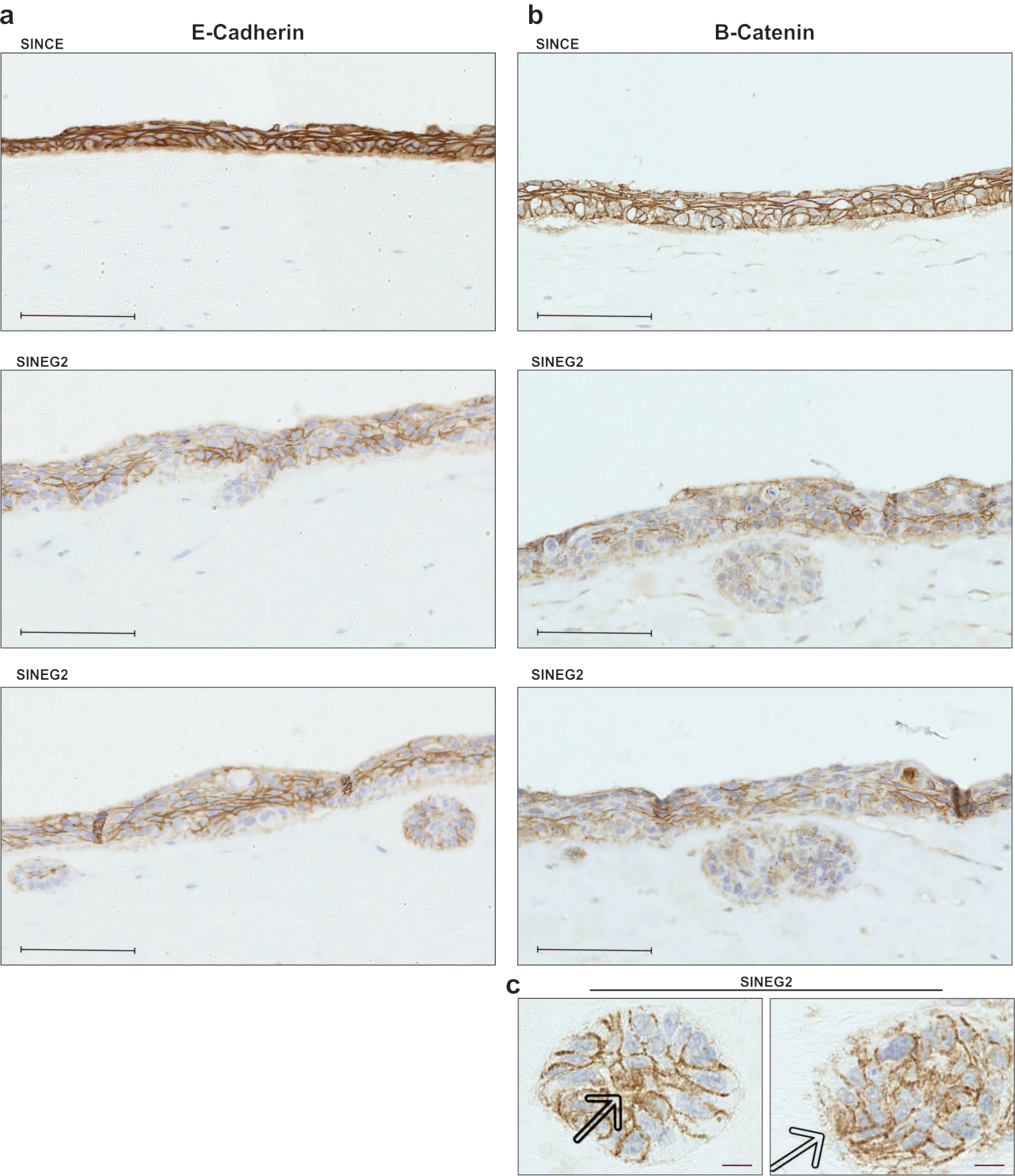
a
E-Cadherin
SINCE
SINEG2
SINEG2
b
B-Catenin
SINCE
SINEG2
SINEG2
c
SINEG2

Figure 6

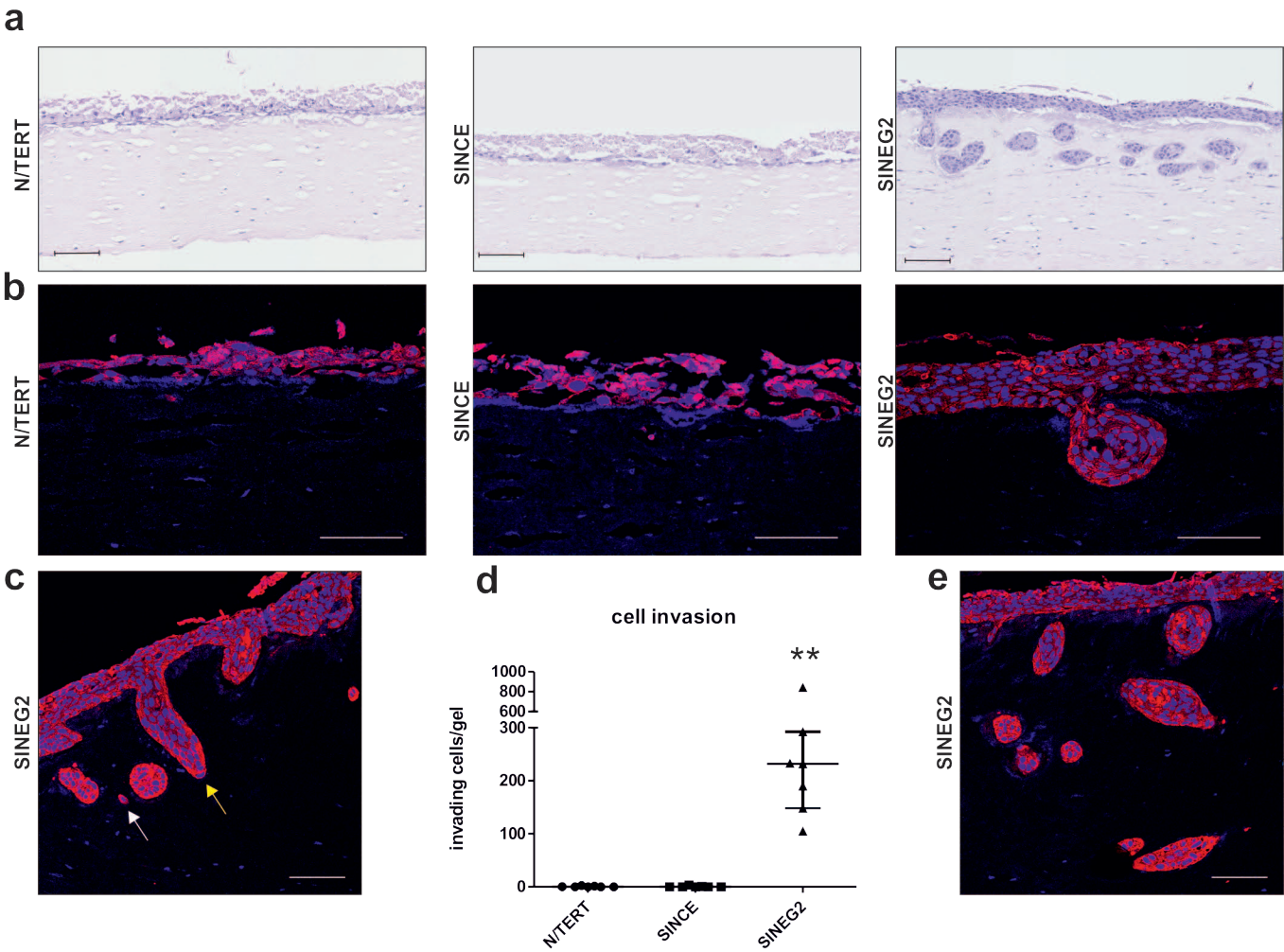
a
N/TERT
SINCE
SINEG2
b
N/TERT
SINCE
SINEG2
c
SINEG2
d
cell invasion
invading cells/gel
1000
800
600
300
200
100
0
**
N/TERT
SINCE
SINEG2
e
SINEG2

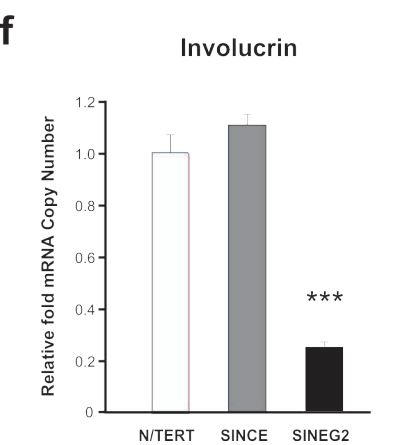
f
Involucrin
Relative fold mRNA Copy Number
1.2
1.0
0.8
0.6
0.4
0.2
0
***
N/TERT
SINCE
SINEG2

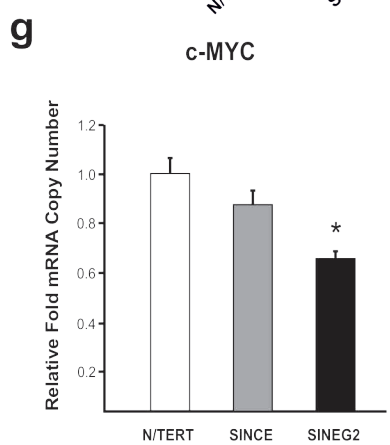
g
c-MYC
Relative Fold mRNA Copy Number
1.2
1.0
0.8
0.6
0.4
0.2
*
N/TERT
SINCE
SINEG2

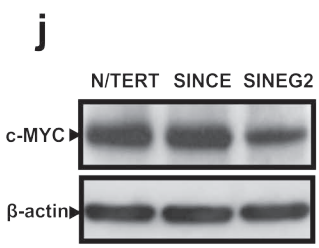
j
N/TERT
SINCE
SINEG2
c-MYC
β-actin

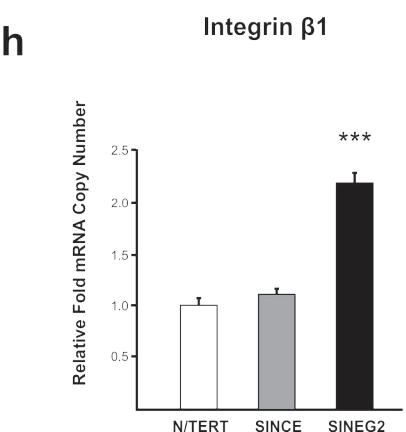
h
Integrin β1
Relative Fold mRNA Copy Number
2.5
2.0
1.5
1.0
0.5
***
N/TERT
SINCE
SINEG2

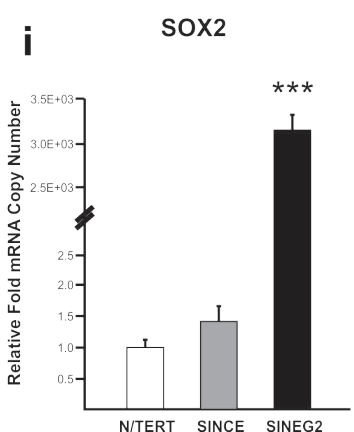
i
SOX2
Relative Fold mRNA Copy Number
3.5E+03
3.0E+03
2.5E+03
2.5
2.0
1.5
1.0
0.5
***
N/TERT
SINCE
SINEG2

Figure S1

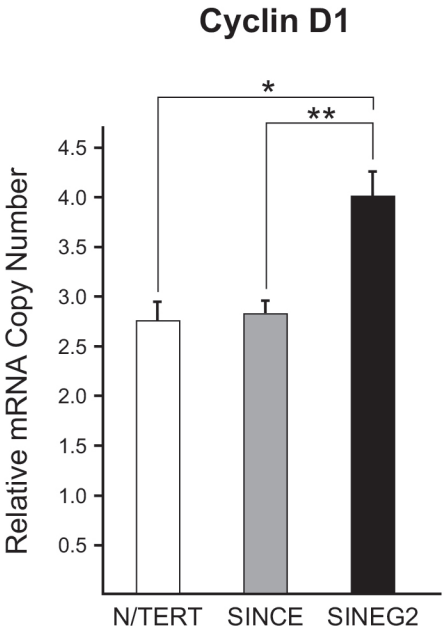
Cyclin D1
*
**
Relative mRNA Copy Number
4.5
4.0
3.5
3.0
2.5
2.0
1.5
1.0
0.5
N/TERT
SINCE
SINEG2

Figure S2

a

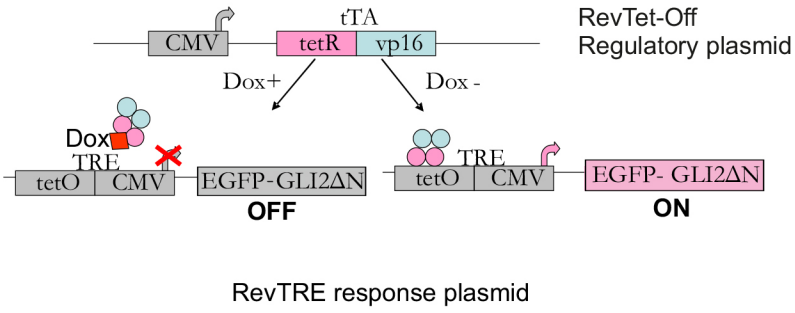

b

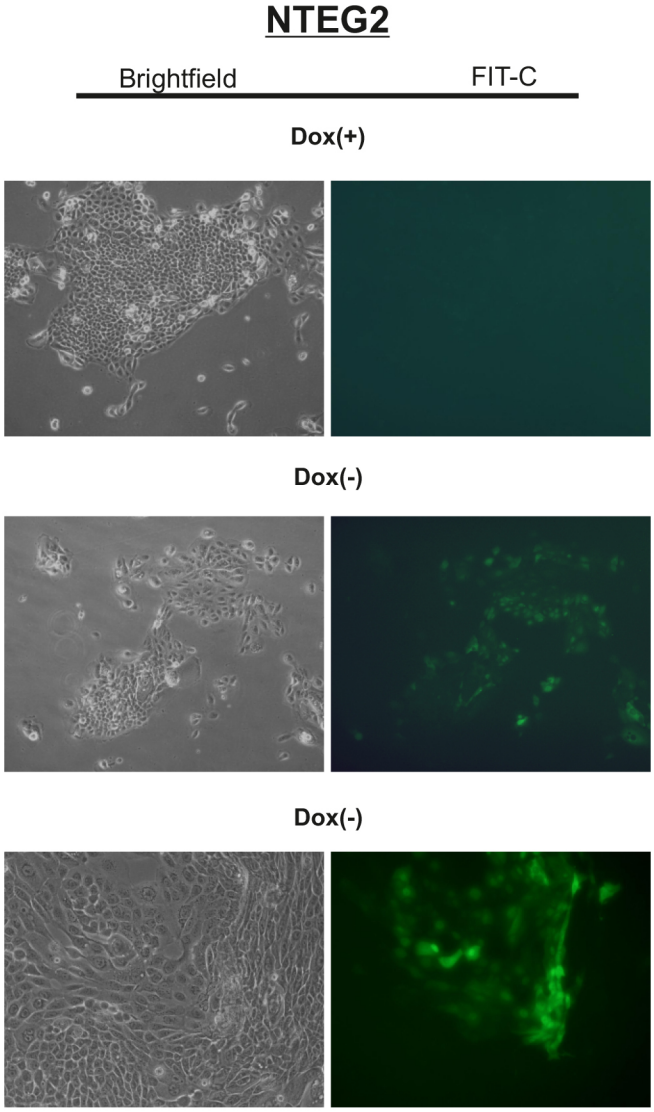

c

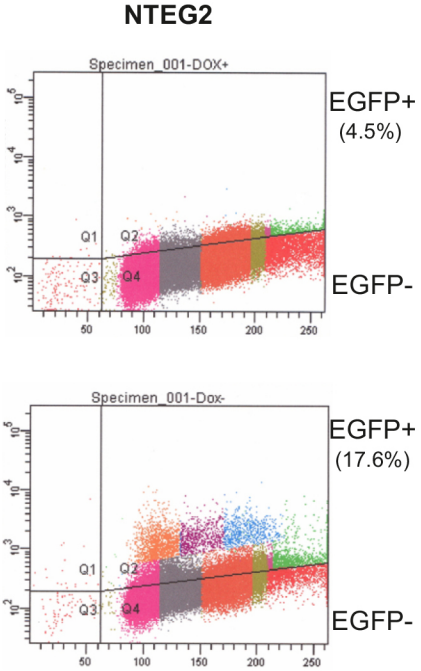

d

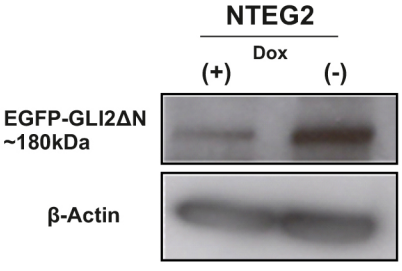

Figure S3

a

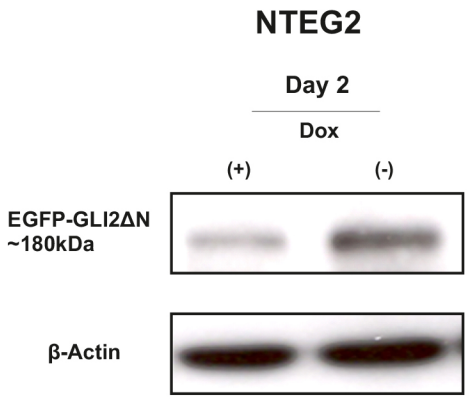

b

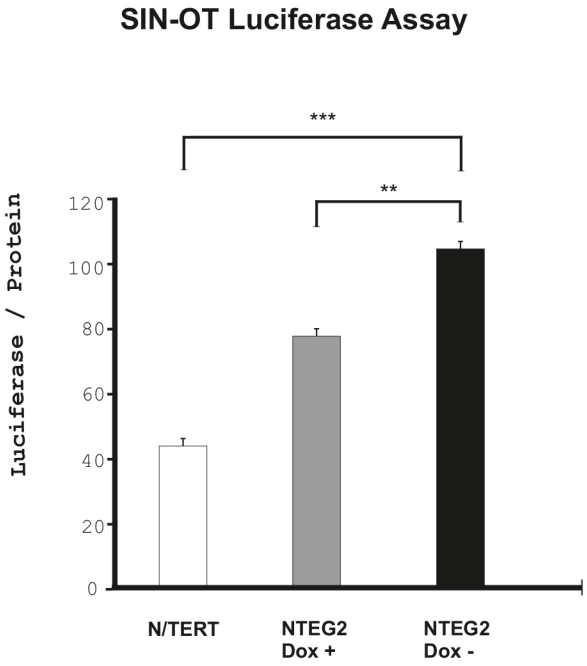

c

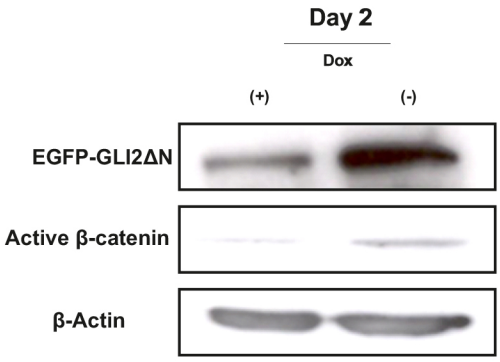

Figure S4

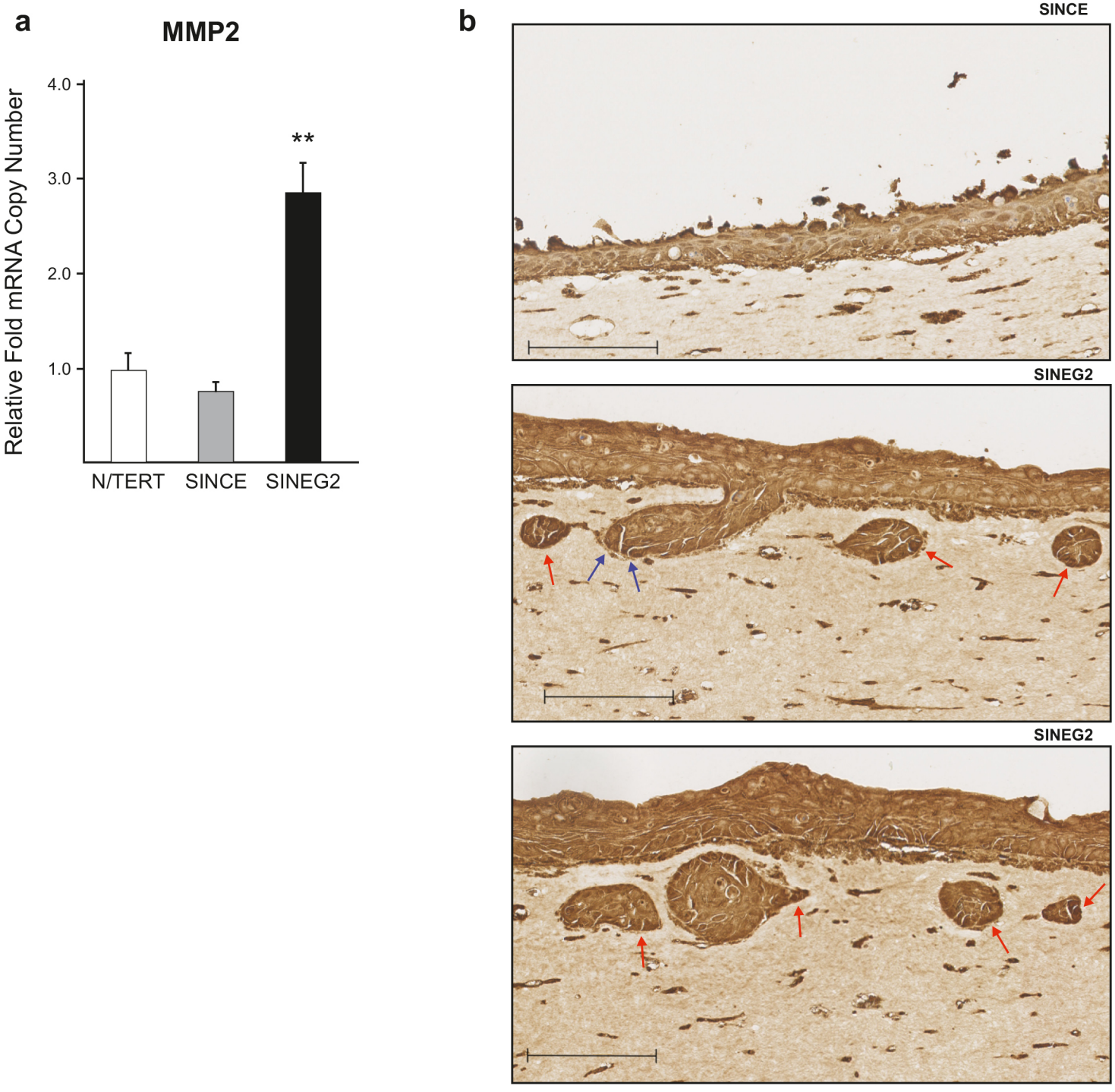
a
MMP2
Relative Fold mRNA Copy Number
4.0
3.0
2.0
1.0
**
N/TERT
SINCE
SINEG2
b
SINCE
SINEG2
SINEG2

Figure S5

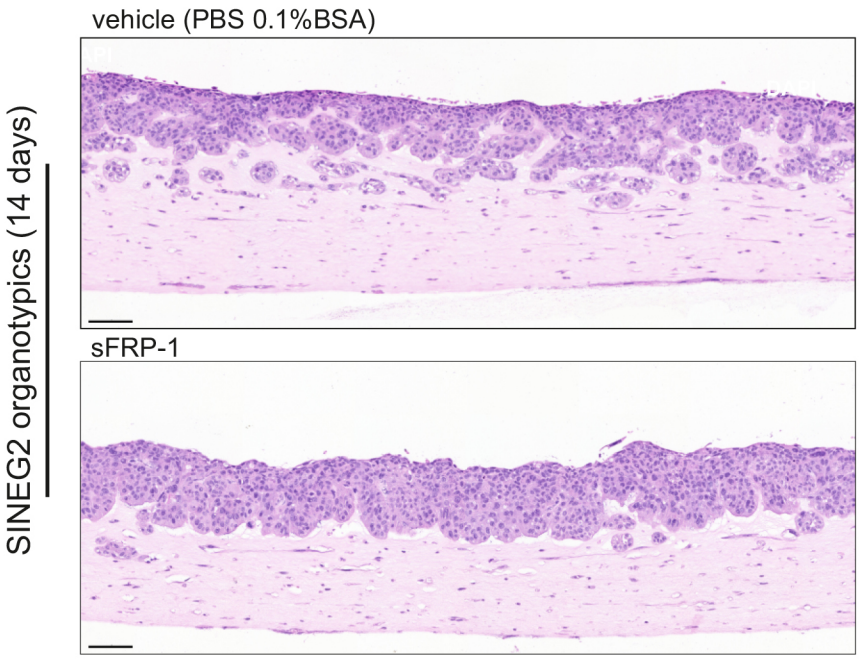

Supplementary Material

Supplementary Table

Table S1: Real-time quantitative PCR primers

Genes	Forward (F) and Reversed (R) Primer Nucleotide Sequence (5'-3')	Product (bp)
c-MYC-F **c-MYC-R**	TTTTTCGGGTAGTGGAAAACC GAGGTCATAGTTCCTGTTGGTG	80
Cyclin D1-F **Cyclin D1-R**	TGTCCTACTACCGCCTCACA CAGGGCTTCGATCTGCTC	92
E-CADHERIN-F **E-CADHERIN-R**	*N/A. Commercially available by Qiagen, West Sussex, UK Cat. No: QT00080143	84
Integrin β1-F **Integrin β1-R**	CGATGCCATCATGCAAGT AGTGAAACCCGGCATCTG	95
IVL-F **IVL-R**	TGCCTGAGCAAGAATGTGAG TTCCTCATGCTGTTCCCAGT	83
MMP2-F **MMP2-R**	*N/A. Commercially available by Qiagen, West Sussex, UK Cat. No: QT00088396	95
POLR2A-F **POLR2A-R**	GCAAATTCACCAAGAGAGACG CACGTCGACAGGAACATCAG	72
SNAIL1-F **SNAIL1-R**	GCTGCAGGACTCTAATCCAGA ATCTCCGGAGGTGGGATG	84
SNAIL2-F **SNAIL2-R**	ACAGCGAACTGGACACACAT GATGGGGCTGTATGCTCCT	113
SOX2-F **SOX2-R**	GGGGGAATGGACCTTGTATAG GCAAAGCTCCTACCGTACCA	85

WNT11-F **WNT11-R**	TGTGCTATGGCATCAAGTGG GCACCTGTGCAGACACCA	108
WNT5A-F **WNT5A-R**	*N/A. Commercially available by Qiagen, West Sussex, UK Cat. No: QT00025109	105
WNT7A-F **WNT7A-R**	GGGACTATGAACCGGAAAGC CCAGAGCTACCACTGAGGAGA	103
YAP1-F **YAP1-R**	CCCAGATGAACGTCACAGC GATTCTCTGGTTCATGGCTGA	82

* N/A: Not applicable

Table S2: Western blot antibodies

Antigen	Supplier and Antibody (Cat. No)
Active-β-catenin	Anti-Active-β-catenin (anti-ABC), clone 8E7, 05-665, mouse monoclonal, Upstate, Lake Placid, NY, USA
β-actin	Anti-β-actin (AC-15) A1978, mouse monoclonal, Sigma-Aldrich, Dorset, UK
β-catenin	Anti-beta-catenin 13-8400, mouse monoclonal, Zymed, San Fransisco, CA, USA
c-MYC	Anti-c-MYC (9E10) sc-40, mouse monoclonal, Santa Cruz, Heidelberg, Germany
E-cadherin	Anti-E-cadherin (HECD-1) ab1416, mouse monoclonal, Abcam, Cambridge, UK
EGFP	Anti-EGFP ab-290, rabbit polyclonal, Abcam, Cambridge, UK
GAPDH	Anti-GAPDH ab9485, rabbit polyclonal, Abcam, Cambridge, UK
Lamin-β1	Anti-Lamin-β1 IMG-5133A, rabbit polyclonal, Imgenex, San Diego, CA, USA

Secondary HRP antibodies were as follows: polyclonal rabbit anti-mouse immunoglobulin/HRP (DakoCytomation, Cambridgeshire, UK) and polyclonal goat anti-rabbit immunoglobulin/HRP (DakoCytomation, Cambridgeshire, UK).

Supplementary Material and Methods

Plasmids and cloning

The pCMV-EGFP-GLI2ΔN expression vector was a kind gift of Prof. Fritz Aberger (Department of Molecular Biology, University of Salzburg, Austria). The pSIN-CMV-EGFP plasmid (Deng et al. , 1997), was kindly provided by Prof. Paul Khavari (Stanford University School of Medicine, CA). The pSIN-MCS vector, containing an MCS insert, was cloned from pSIN-CMV-EGFP plasmid (Deng, Lin, 1997). The pSIN-CMV-GLI2ΔN stable expression retroviral transduction vector was obtained as previously described (Pantazi, Gemenetzidis, 2014). The retroviral regulatory tTA vector (pRevTet-Off) and the retroviral response cloning vector (pRev-TRE) were all purchased from Clontech Laboratories, Palo Alto, CA as part of the Rev Tet-Off System (Chang et al. , 2000, Chi et al. , 2005). The pTRE-CMV-EGFP-GLI2ΔN inducible expression retroviral transduction vector was obtained by introducing a BamHI site between the NheI and EcoRV sites in pCMV-EGFP-GLI2ΔN by a linker oligonucleotide, excising the ORF with BamHI and subcloning it into the pRevTRE vector cut with BamHI. The Tcf-4 responsive luciferase plasmid pGL3-OT (OT-β-catenin responsive promoter), an improved version of TOPFLASH (Shih, Yu, 2000), which contains the TCF-4 binding sites (He, Sparks, 1998, Korinek et al. , 1997, Shih, Yu, 2000) was kindly provided by Bert Vogelstein (The John Hopkins Oncology Centre Baltimore, MD). The pSIN-OT-Luciferase (pSIN-OT-Luc) reporter transduction vector was obtained by excising the OT-Luc cassette from pGL3-OT, with XmaI, NgoMIV and subcloning it into the NgoMIV linearized pSIN-MCS.

Cell lines and culture

PT67 packaging cells, derived from an NH/3H3-based line expressing the 10A1 virus envelope, were purchased from (Clontech) as part of the Rev Tet-Off System (Chang, Jakobi, 2000, Chi, Chen, 2005) and cultured similarly to Phoenix cells as previously describe described (Pantazi, Gemenetzidis, 2014). The N/TERT RevTRE-CMV-EGFP-GLI2ΔN inducible cell line, referred to as NTEG2 cell line, was prepared as recommended by the kit manufacturer (RevTet-Off System, Clontech) (Chang, Jakobi, 2000, Chi, Chen, 2005). The retrovirus-mediated tet-regulated gene expression system (RevTet-Off) (Clontech) combines the advantages of retroviral transfer with those of tet-regulation and thus allows efficient and tight quantitative and temporal control of gene expression. In the RevTet-Off system, transcription of the gene of interest (in this study EGFP-GLI2ΔN fusion gene) is turned off in the presence of doxycycline (Dox) (a derivative of tetracycline) (NTEG2 Dox+), while transcription of this gene (EGFP-GLI2ΔN fusion gene) is turned on in the absence of doxycycline (NTEG2 Dox-). NTEG2 cells were maintained in RM+ growth media (DMEM supplemented with 25% (v/v) Ham's F12 medium (PAA), 10% (v/v) FCS (Biosera), 1% (v/v) Glutamine (PAA), 1% (v/v) penicillin/streptomycin (PAA), various mitogens (0.4μg/ml hydrocortisone (Sigma-Aldrich), 0.1nM cholera toxin (BioMol, Exeter, UK), 5μg/ml transferrin (Sigma), 20pM liothyronine (Sigma), 5μg/ml insulin (Sigma) and 10ng/ml epidermal growth factor (AbD Serotec, Kidlington, UK), in the presence of 50μg/ml Hygromycin B (Clontech) and 250μg/ml G418 (Clontech) and kept under Doxycycline (40ng/ml) (Clontech) repression for maintenance and characterisation studies. Due to the heterogeneity of the cell population, a higher concentration of Dox (10μg/ml) (Clontech)

was used to maximize repression in subsequent experiments. To induce expression cells were cultured in the absence of doxycycline in a medium containing 10% (v/v) Tet System Approved fetal bovine serum (Clontech). Thus, when doxycycline was removed, the inducible cell line (NTEG2 Dox-) was cultured in DMEM supplemented with 25% (v/v) Ham's F12 medium (PAA), 10% (v/v) Tet System Approved fetal bovine serum (Tet-FBS) (Clontech), 1% (v/v) glutamine (PAA), 1% (v/v) penicillin/streptomycin (PAA), 50µg/ml Hygromycin B (Clontech) and 250µg/ml G418 (Clontech) and various mitogens (0.4µg/ml hydrocortisone (Sigma), 0.1nM cholera toxin (BioMol), 5µg/ml transferrin (Sigma), 20pM liothyronine (Sigma), 5µg/ml insulin (Sigma) and 10ng/ml epidermal growth factor (AbD Serotec). All cells were grown at 37^{o}C in a humidified atmosphere of 10% (v/v) CO_2/90% (v/v) air. NTEG2 Dox- cells were further selected by FACS sorting and cultured under the presence of doxycycline, until required. NTEG2 cells were further transduced with the pSIN-OT-Luciferase (pSIN-OT-Luc) retroviral plasmid, to produce the reporter inducible cell line (NTEG2-OTLuc). The reporter inducible cell line was then cultured in RM+ growth medium, containing 50µg/ml Hygromycin B (Clontech), 250µg/ml G418 (Clontech), and kept under Doxycycline (Clontech) repression until required for experiments. All cells were grown at 37^{o}C in a humidified atmosphere of 10% (v/v) CO_2/90% (v/v) air.

Retroviral Infection

N/TERT cells were stably transduced with retroviruses encoding pRevTRE-CMV-EGFP-GLI2ΔN and pRevTet-Off plasmids, according to the kit manufacturer (RevTet-Off System, Clontech) (Chang, Jakobi, 2000, Chi, Chen, 2005) and

as previously described in Pantazi et al 2014 (Pantazi, Gemenetzidis, 2014) to yield the N/TERT RevTRE-CMV-EGFP-GLI2ΔN (NTEG2) inducible cell line. Retroviral supernatant was obtained as previously described (Pantazi, Gemenetzidis, 2014), but using PT67 packaging cell line (Clontech) (Miller and Chen, 1996), instead of Phoenix A packaging cells. Briefly, N/TERT cells were pre transduced with the regulatory vector pRevTet-Off (Clontech), to yield the founder cell line NT-TetOff. The founder cell line was selected with 500µg/ml G418 (Clontech), and then transduced with the expression vector pRevTRE-CMV-EGFP-GLI2ΔN (RevTRE response plasmid) and selected with 100µg/ml Hygromycin B (Clontech), to yield the NTEG2 inducible cell line. All transductions using pSIN based constructs were carried out as previously described (Pantazi, Gemenetzidis, 2014).

Luciferase Reporter Assay

In this study, the pGL3-OT was cloned into pSIN retroviral vector and luciferase was used to detect and measure the activity of the OT promoter, and indirectly the transcriptional activity of β-catenin (pSIN-OT-Luciferase). NTERT, SINCE, SINEG2 cells were transduced with pSIN-OT-Luciferase (pSIN-OT-Luc) retroviral plasmid, and were left to express the transgene for 72h prior to harvesting for luciferase activity and protein content measurement. NTERT, SINEG2, SINCE transduced cells were split and seeded in 6-well plates (16.8×10^4cells/well) 48h after viral infection and the next day (72h post-infection) cells were lysed and examined for luciferase activity and protein content. Similarly, N/TERT and NTEG2 cells were transduced with pSIN-OT-Luciferase (pSIN-OT-Luc) retroviral plasmid, and were left to express the transgene for 5 days prior to harvesting for

luciferase activity and protein content measurement. N/TERT and NTEG2 transduced cells were split and seeded in 6-well plates ($4.2x10^4$ cells/well) 48h after viral infection and the next day (72h post-infection) doxycycline was removed from transduced cells for another 48hr (NTEG2 Dox-). Day 5 post-transduction, cells were lysed and examined for luciferase activity and protein content. All cell lysates were prepared using the Reporter 1x Lysis Buffer (Promega) and assayed for protein content and luciferase activity using the Bio-Rad Protein Assay System (BioRad, Hertfordshire, UK) and the Bright-Glo™ Luciferase Assay System (Promega) respectively, according to manufacturer's protocol. Luminescence values were determined using a FLUOSTAR OPTIMA microplate reader (BMG LABTECH, Aylesbury, UK). Luminescence data of each sample were normalized to protein content (luciferase/μg).

Organotypic cultures

NTERT, SINCE and SINEG2 cells were grown with dermal human fibroblasts in organotypic 3D cultures, under conditions that support the proliferation and differentiation of epidermal keratinocytes and mimic their *in vivo* pattern of growth and differentiation. Briefly, collagen gels were prepared by mixing 7 volumes of collagen/matrigel (75% Collagen type I and 25% Matrigel, BD Bioscience) with 1 volume 10× DMEM (Invitogen, Paisley, UK), 1 volume FCS (Biosera), and 1 volume FGM in which HFF had been suspended at a concentration of 5×10^6/ml. Then 1ml of this solution (0.5×10^6 HFF) was aliquoted into wells of a 24-well plate and allowed to polymerise for 30 min at 37 ◦C. After polymerization, 1ml of FGM was added per well and gels were left for 18 h at 37◦C to equilibrate or $0.5x10^6$ of either N/TERT or SINCE or SINEG2 keratinocytes suspended

in 1ml of RM+ growth medium were seeded on top of each collagen gel. After 24h, gels were removed from the 24-well plates and placed on to individual collagen coated nylon discs resting on steel grids placed in six-well plates. Sufficient RM+ growth medium was added to reach the lower surface of the grid allowing the epithelial layer to grow at an air-liquid interface. Medium was changed every 2 days. Gels were harvested at day 14 and day 28 and fixed in 4% formaldehyde (Sigma) overnight. The organotypic cultures were bisected vertically and embedded in paraffin wax on their cut surface for sectioning. 4μm sections were cut from the organotypic cultures paraffin blocks and transferred to charged microscope slides for H&E or immuno- staining, to determine the invasion index, protein expression, as well as any phenotypic changes. Organotypic culture processing (wax embedding), sectioning, and H&E staining were all occurred at the Pathology Department of the Institute of Cancer, Barts and the London School of Medicine and Dentistry, Charterhouse square, London, UK. The H&E stained slides were imaged on the NanoZoomer Digital Pathology (NDP) whole slide scanner (Hamamatsu Photonics UK Limited, Hertfotdsire, UK), in brightfield mode and images were processed and analyzed using the Viewing Software NDP.view2 U12388-01.

Cytokeratin Immnunofluorescence in organotypic cultures

Briefly, paraffin embedded organotypic raft sections were initially heated at 60°C for 10 minutes and were then deparaffinised in Xylene (2×5 minutes) and dehydrated (100% ethanol (2x), 90% ethanol, 70% ethanol, 50% ethanol for 5 minutes each) prior to rehydrated in distilled water (5 minutes). Antigen unmasking was performed by incubation in sub-boiling temperature for 20 minutes in antigen retrieval solution (pH 6.0;

DakoCytomation). The sections were washed twice in PBS and blocked by 5% goat serum (Sigma) in PBS (PAA) with 0.05% Tween-20 (T) (Sigma) and 0.1% BSA (PAA) for 1 hour at room temperature (RT). Incubation with primary antibody in 1x PBS/0.05% T/0.1% BSA was performed for 2 hours at RT or overnight at 4°C. Sections were washed 3x5 minutes in 1x PBS/T, prior to incubation with Alexa Fluor 568 goat anti-mouse IgG (H+L) secondary antibody (Invitrogen) at 1:500 dilution in 1x PBS/0.05% T/0.1% BSA, for 1 hour at RT. Finally, sections were washed 3x5 minutes in 1x PBS/T and mounted with Prolong Gold Antifade Reagent Solution containing DAPI dilactate (Invitrogen).

Sectioning and Immunohistochemistry analysis in 3D cultures

Sectioning, immunostaining and imaging were performed at the Blizard Core Pathology Department, Queen Mary University of London, according to local standard protocols. Briefly, immunohistochemistry was carried out on 4µm sections (cut from the organotypic cultures processed in paraffin blocks) that were mounted on electrically charged slides (VWR, Leicestershire, UK) and dried overnight in a 60°C oven. The sections were stained on a DAKO Autostainer with the DAKO Flex+ Envision high pH Kit (K8012, DakoCytomation). The sections were antigen retrieved in the DAKO link machine (using the high pH from the kit above and at the factory settings) and then stained on the DAKO autostainer where the slides are treated with H_2O_2, primary antibody, linker, polymer secondary and visualised with DAB; all components (except primary antibodies) are from the kit and used at the times recommended. The sections were then counterstained with Gills Haematoxylin (In house preparation), dehydrated and cleared on a Gemini

Autostainer (Thermo Fisher, Leicestershire, UK) and cover-slipped with a xylene based mountant.

Supplementary Results

Generation and characterization of the inducible NTEG2 cell line

The preparation of the inducible cell line NTEG2 was based on the RevTet-OFF regulatory system, which allows efficient and tight quantitative and temporal control of gene expression. With this inducible system the transcription of the gene of interest (in this study EGFP-GLI2ΔN fusion gene) is turned off in the presence of doxycycline (Dox) (NTEG2 Dox+), while transcription of this gene (EGFP-GLI2ΔN fusion gene) is turned on in the absence of doxycycline (NTEG2 Dox-) (Supplementary Figure S2a). For the generation of the NTEG2 cell line we used heterogeneous cell populations in order to avoid any clone specific effects. Following drug selection and induction, NTEG2 cells were FACS sorted, and all EGFP+ cells were collected using N/TERT as a reference cell line to obtain baseline values of green fluorescence, replated and cultured under the presence of doxycycline.

Significant induction of protein levels was evidenced under fluorescent microscopy, 5 days after Dox removal (Supplementary Figure S2b; Dox(-) panels), while no induction of EGFP-GLI2ΔN fusion protein was observed in NTEG2 cells under the presence of doxycycline (Supplementary Figure S2b; Dox(+) panel). Flow cytometry analysis of NTEG2 cells showed an increased percentage of EGFP+ cells when Dox was removed, but also a small baseline induction of fluorescence even in Dox treated cells (Supplementary Figure S2c). Immunoblotting for EGFP-GLI2ΔN fusion protein confirmed GLI2ΔN induction in NTEG2 cells upon removal of Dox in comparison with baseline leak (Supplementary Figure S2d). Because we used pooled (FACS sorted EGFP+) NTEG2 cells, variation was observed in the levels of GLI2ΔN expression (EGFP intensity) between

different clones in NTEG2 culture (Supplementary Figure S2b compare the two lower Dox(-) panels). To control for this variation we always measured levels of EGFP-GLI2ΔN induction/suppression by flow cytometry and immunoblotting prior to carrying out experiments to ensure similar levels of GLI2ΔN expression between experiments.

Supplementary Figure Legends

Figure S1. Cyclin-D1 expression in GLI2ΔN-expressing keratinocytes. RNA was harvested from N/TERT, SINCE, and SINEG2 cells to examine the levels of Cyclin-D1 mRNA expression. Quantitative RT-PCR analysis showed an increase in the expression of Cyclin-D1 in SINEG2 cells compared to N/TERT and SINCE control cells. Each bar represents a mean ± s.e.m of triplicate samples. * $P \leq 0.05$, ** $P \leq 0.01$.

Figure S2. Generation and characterization of NTEG2 inducible cell line. (a) Diagram illustrating the principle of induction and/or repression of EGFP-GLI2ΔN fusion protein under the control of Doxycycline. Tetracycline controlled transactivator (tTa) binds to tetracycline response element (TRE) to activate transgene transcription mediated by the CMV promoter in the absence of doxycycline. tTa binding is repressed in the presence of doxycycline. **(b)** Representative pictures of NTEG2 cells in the presence (Dox(+)) or absence (Dox(-)) of doxycycline. Varying levels of EGFP-GLI2ΔN expression were observed possibly due to the heterogeneity of NTEG2 cell population. **(c)** Flow cytometry analysis of NTEG2 cell line in the presence or absence of doxycycline. Clear induction of EGFP-GLI2ΔN is shown in Dox(-) cells while background activity of EGFP-GLI2ΔN is also evidenced in the presence of doxycycline (top panel; Q2 quartile) represented by the small population detected above threshold levels of fluorescence obtained from wild-type N/TERT cells. **(d)** Immunoblotting analysis of NTEG2 cells in the presence or absence (5 days) of doxycycline against anti-EGFP antibody (EGFP-GLI2ΔN fusion protein ~ 180kDa), with β-actin (~ 42kDa) used as loading control. Significant induction of the

transgene is observed in Dox(-) cells, while background levels of induction are also present, as evidenced by previous flow cytometry analysis.

Figure S3. GLI2ΔN induces β-catenin transcriptional activation. (a) Immunoblotting in NTEG2 inducible cell line against EGFP antibody (EGFP-GLI2ΔN fusion protein ~180kDa), in the presence or absence of doxycycline, for 48h. β-actin (~42kDa) was used as loading control. Results indicated high levels of EGFP-GLI2ΔN fusion protein inducibility before the experiment. 48h of doxycycline withdrawal was the time-point of choice in order to achieve significant induction of EGFP-GLI2ΔN and maximum expression of SIN-OT-Luc reporter vector. **(b)** Luciferase assay on N/TERT and NTEG2 induced and uninduced cells. N/TERT keratinocytes were used as internal controls, due to background levels of GLI2ΔN in Dox+ NTEG2 cells. N/TERT and NTEG2 cells were transduced with SIN-OT-Luciferase vector and expressed the transgene for 72h, followed by doxycycline removal for another 48h. Day 5 post-transduction, lysates were prepared and examined for luciferase activity and protein content. OT-β-catenin responsive promoter was significantly activated in NTEG2 Dox- cells (~ 2.4 fold) compared to both N/TERT (*** $P \leq 0.001$) and NTEG2 Dox+ (** $P \leq 0.01$) cells. The increase in luciferase activity observed in uninduced NTEG2 cells (NTEG2 Dox+), compared to N/TERT cells can possibly be attributed to incomplete repression of GLI2ΔN in the presence of Dox. Each bar represents a mean ± s.e.m of normalised to protein content triplicate samples. **(c)** Active (dephosphorylated) β-catenin levels are increased in induced NTEG2 cells compared to the uninduced control cells. Active β-catenin levels in cell lysates from induced and uninduced NTEG2 cells were analysed by immunoblotting with anti-active-

β-catenin antibody (~92kDa). The EGFP-GLI2ΔN protein levels after 48h removal of doxycycline are also shown for reference and β-actin was used as loading control.

Figure S4. MMP2 expression in GLI2ΔN-expressing keratinocytes. (a) RNA was harvested from N/TERT, SINCE, and SINEG2 cells to examine the levels of MMP2 mRNA expression. qRT-PCR analysis showed an increase in the expression of MMP2 in SINEG2 cells compared to N/TERT and SINCE control cells. Each bar represents mean fold induction relative to N/TERT (arbitrary value of 1) ± s.e.m of triplicate samples.** $P \leq 0.01$. **(b)** Immuno-histochemical staining for MMP2 in sections of organotypic cultures of control SINCE cells (top panel) and SINEG2 cells (lower two panels) grown in collagen/matrigel gels for 14 days. Increased MMP2 expression is seen in SINEG2 cells compared to SINCE control cells, and shows a more pronounced staining in the edges/periphery of the invading multicellular strands with a bud-like tip (blue arrow) and clusters (red arrow). Scale bar: 100μm.

Figure S5. sFRP-1 blocks invasion of SINEG2 cells. 14-days organotypic cultures of SINEG2 cells treated with vehicle (top panel) or 0.1 μg/ml sFRP-1 (bottom panel). SIENG2 cells produce a thick basal-like undifferentiated epithelium in both conditions. When treated with vehicle only (top panel), SINEG2 cells display significant invasion capacity with clusters of cells invading the tissue, whereas treatment with sFRP-1 (bottom panel) reduces the capacity of SINEG2 cells to detach from the main bulk of the epithelium and invade into the organotypic ECM.

Supplementary Material

Supplementary Table

Table S1: Real-time quantitative PCR primers

Genes	Forward (F) and Reversed (R) Primer Nucleotide Sequence (5'-3')	Product (bp)
c-MYC-F **c-MYC-R**	TTTTTCGGGTAGTGGAAAACC GAGGTCATAGTTCCTGTTGGTG	80
Cyclin D1-F **Cyclin D1-R**	TGTCCTACTACCGCCTCACA CAGGGCTTCGATCTGCTC	92
E-CADHERIN-F **E-CADHERIN-R**	*N/A. Commercially available by Qiagen, West Sussex, UK Cat. No: QT00080143	84
Integrin β1-F **Integrin β1-R**	CGATGCCATCATGCAAGT AGTGAAACCCGGCATCTG	95
IVL-F **IVL-R**	TGCCTGAGCAAGAATGTGAG TTCCTCATGCTGTTCCCAGT	83
MMP2-F **MMP2-R**	*N/A. Commercially available by Qiagen, West Sussex, UK Cat. No: QT00088396	95
POLR2A-F **POLR2A-R**	GCAAATTCACCAAGAGAGACG CACGTCGACAGGAACATCAG	72
SNAIL1-F **SNAIL1-R**	GCTGCAGGACTCTAATCCAGA ATCTCCGGAGGTGGGATG	84
SNAIL2-F **SNAIL2-R**	ACAGCGAACTGGACACACAT GATGGGGCTGTATGCTCCT	113
SOX2-F **SOX2-R**	GGGGGAATGGACCTTGTATAG GCAAAGCTCCTACCGTACCA	85

WNT11-F **WNT11-R**	TGTGCTATGGCATCAAGTGG GCACCTGTGCAGACACCA	108
WNT5A-F **WNT5A-R**	*N/A. Commercially available by Qiagen, West Sussex, UK Cat. No: QT00025109	105
WNT7A-F **WNT7A-R**	GGGACTATGAACCGGAAAGC CCAGAGCTACCACTGAGGAGA	103
YAP1-F **YAP1-R**	CCCAGATGAACGTCACAGC GATTCTCTGGTTCATGGCTGA	82

* N/A: Not applicable

Table S2: Western blot antibodies

Antigen	Supplier and Antibody (Cat. No)
Active-β-catenin	Anti-Active-β-catenin (anti-ABC), clone 8E7, 05-665, mouse monoclonal, Upstate, Lake Placid, NY, USA
β-actin	Anti-β-actin (AC-15) A1978, mouse monoclonal, Sigma-Aldrich, Dorset, UK
β-catenin	Anti-beta-catenin 13-8400, mouse monoclonal, Zymed, San Fransisco, CA, USA
c-MYC	Anti-c-MYC (9E10) sc-40, mouse monoclonal, Santa Cruz, Heidelberg, Germany
E-cadherin	Anti-E-cadherin (HECD-1) ab1416, mouse monoclonal, Abcam, Cambridge, UK
EGFP	Anti-EGFP ab-290, rabbit polyclonal, Abcam, Cambridge, UK
GAPDH	Anti-GAPDH ab9485, rabbit polyclonal, Abcam, Cambridge, UK
Lamin-β1	Anti-Lamin-β1 IMG-5133A, rabbit polyclonal, Imgenex, San Diego, CA, USA

Secondary HRP antibodies were as follows: polyclonal rabbit anti-mouse immunoglobulin/HRP (DakoCytomation, Cambridgeshire, UK) and polyclonal goat anti-rabbit immunoglobulin/HRP (DakoCytomation, Cambridgeshire, UK).

Supplementary Material and Methods

Plasmids and cloning

The pCMV-EGFP-GLI2ΔN expression vector was a kind gift of Prof. Fritz Aberger (Department of Molecular Biology, University of Salzburg, Austria). The pSIN-CMV-EGFP plasmid (Deng et al. , 1997), was kindly provided by Prof. Paul Khavari (Stanford University School of Medicine, CA). The pSIN-MCS vector, containing an MCS insert, was cloned from pSIN-CMV-EGFP plasmid (Deng, Lin, 1997). The pSIN-CMV-GLI2ΔN stable expression retroviral transduction vector was obtained as previously described (Pantazi, Gemenetzidis, 2014). The retroviral regulatory tTA vector (pRevTet-Off) and the retroviral response cloning vector (pRev-TRE) were all purchased from Clontech Laboratories, Palo Alto, CA as part of the Rev Tet-Off System (Chang et al. , 2000, Chi et al. , 2005). The pTRE-CMV-EGFP-GLI2ΔN inducible expression retroviral transduction vector was obtained by introducing a BamHI site between the NheI and EcoRV sites in pCMV-EGFP-GLI2ΔN by a linker oligonucleotide, excising the ORF with BamHI and subcloning it into the pRevTRE vector cut with BamHI. The Tcf-4 responsive luciferase plasmid pGL3-OT (OT-β-catenin responsive promoter), an improved version of TOPFLASH (Shih, Yu, 2000), which contains the TCF-4 binding sites (He, Sparks, 1998, Korinek et al. , 1997, Shih, Yu, 2000) was kindly provided by Bert Vogelstein (The John Hopkins Oncology Centre Baltimore, MD). The pSIN-OT-Luciferase (pSIN-OT-Luc) reporter transduction vector was obtained by excising the OT-Luc cassette from pGL3-OT, with XmaI, NgoMIV and subcloning it into the NgoMIV linearized pSIN-MCS.

Cell lines and culture

PT67 packaging cells, derived from an NH/3H3-based line expressing the 10A1 virus envelope, were purchased from (Clontech) as part of the Rev Tet-Off System (Chang, Jakobi, 2000, Chi, Chen, 2005) and cultured similarly to Phoenix cells as previously describe described (Pantazi, Gemenetzidis, 2014). The N/TERT RevTRE-CMV-EGFP-GLI2ΔN inducible cell line, referred to as NTEG2 cell line, was prepared as recommended by the kit manufacturer (RevTet-Off System, Clontech) (Chang, Jakobi, 2000, Chi, Chen, 2005). The retrovirus-mediated tet-regulated gene expression system (RevTet-Off) (Clontech) combines the advantages of retroviral transfer with those of tet-regulation and thus allows efficient and tight quantitative and temporal control of gene expression. In the RevTet-Off system, transcription of the gene of interest (in this study EGFP-GLI2ΔN fusion gene) is turned off in the presence of doxycycline (Dox) (a derivative of tetracycline) (NTEG2 Dox+), while transcription of this gene (EGFP-GLI2ΔN fusion gene) is turned on in the absence of doxycycline (NTEG2 Dox-). NTEG2 cells were maintained in RM+ growth media (DMEM supplemented with 25% (v/v) Ham's F12 medium (PAA), 10% (v/v) FCS (Biosera), 1% (v/v) Glutamine (PAA), 1% (v/v) penicillin/streptomycin (PAA), various mitogens (0.4μg/ml hydrocortisone (Sigma-Aldrich), 0.1nM cholera toxin (BioMol, Exeter, UK), 5μg/ml transferrin (Sigma), 20pM liothyronine (Sigma), 5μg/ml insulin (Sigma) and 10ng/ml epidermal growth factor (AbD Serotec, Kidlington, UK), in the presence of 50μg/ml Hygromycin B (Clontech) and 250μg/ml G418 (Clontech) and kept under Doxycycline (40ng/ml) (Clontech) repression for maintenance and characterisation studies. Due to the heterogeneity of the cell population, a higher concentration of Dox (10μg/ml) (Clontech)

was used to maximize repression in subsequent experiments. To induce expression cells were cultured in the absence of doxycycline in a medium containing 10% (v/v) Tet System Approved fetal bovine serum (Clontech). Thus, when doxycycline was removed, the inducible cell line (NTEG2 Dox-) was cultured in DMEM supplemented with 25% (v/v) Ham's F12 medium (PAA), 10% (v/v) Tet System Approved fetal bovine serum (Tet-FBS) (Clontech), 1% (v/v) glutamine (PAA), 1% (v/v) penicillin/streptomycin (PAA), 50µg/ml Hygromycin B (Clontech) and 250µg/ml G418 (Clontech) and various mitogens (0.4µg/ml hydrocortisone (Sigma), 0.1nM cholera toxin (BioMol), 5µg/ml transferrin (Sigma), 20pM liothyronine (Sigma), 5µg/ml insulin (Sigma) and 10ng/ml epidermal growth factor (AbD Serotec). All cells were grown at 37ºC in a humidified atmosphere of 10% (v/v) CO_2/90% (v/v) air. NTEG2 Dox- cells were further selected by FACS sorting and cultured under the presence of doxycycline, until required. NTEG2 cells were further transduced with the pSIN-OT-Luciferase (pSIN-OT-Luc) retroviral plasmid, to produce the reporter inducible cell line (NTEG2-OTLuc). The reporter inducible cell line was then cultured in RM+ growth medium, containing 50µg/ml Hygromycin B (Clontech), 250µg/ml G418 (Clontech), and kept under Doxycycline (Clontech) repression until required for experiments. All cells were grown at 37ºC in a humidified atmosphere of 10% (v/v) CO_2/90% (v/v) air.

Retroviral Infection

N/TERT cells were stably transduced with retroviruses encoding pRevTRE-CMV-EGFP-GLI2ΔN and pRevTet-Off plasmids, according to the kit manufacturer (RevTet-Off System, Clontech) (Chang, Jakobi, 2000, Chi, Chen, 2005) and

as previously described in Pantazi et al 2014 (Pantazi, Gemenetzidis, 2014) to yield the N/TERT RevTRE-CMV-EGFP-GLI2ΔN (NTEG2) inducible cell line. Retroviral supernatant was obtained as previously described (Pantazi, Gemenetzidis, 2014), but using PT67 packaging cell line (Clontech) (Miller and Chen, 1996), instead of Phoenix A packaging cells. Briefly, N/TERT cells were pre transduced with the regulatory vector pRevTet-Off (Clontech), to yield the founder cell line NT-TetOff. The founder cell line was selected with 500μg/ml G418 (Clontech), and then transduced with the expression vector pRevTRE-CMV-EGFP-GLI2ΔN (RevTRE response plasmid) and selected with 100μg/ml Hygromycin B (Clontech), to yield the NTEG2 inducible cell line. All transductions using pSIN based constructs were carried out as previously described (Pantazi, Gemenetzidis, 2014).

Luciferase Reporter Assay

In this study, the pGL3-OT was cloned into pSIN retroviral vector and luciferase was used to detect and measure the activity of the OT promoter, and indirectly the transcriptional activity of β-catenin (pSIN-OT-Luciferase). NTERT, SINCE, SINEG2 cells were transduced with pSIN-OT-Luciferase (pSIN-OT-Luc) retroviral plasmid, and were left to express the transgene for 72h prior to harvesting for luciferase activity and protein content measurement. NTERT, SINEG2, SINCE transduced cells were split and seeded in 6-well plates (16.8×10^4cells/well) 48h after viral infection and the next day (72h post-infection) cells were lysed and examined for luciferase activity and protein content. Similarly, N/TERT and NTEG2 cells were transduced with pSIN-OT-Luciferase (pSIN-OT-Luc) retroviral plasmid, and were left to express the transgene for 5 days prior to harvesting for

luciferase activity and protein content measurement. N/TERT and NTEG2 transduced cells were split and seeded in 6-well plates ($4.2x10^4$ cells/well) 48h after viral infection and the next day (72h post-infection) doxycycline was removed from transduced cells for another 48hr (NTEG2 Dox-). Day 5 post-transduction, cells were lysed and examined for luciferase activity and protein content. All cell lysates were prepared using the Reporter 1x Lysis Buffer (Promega) and assayed for protein content and luciferase activity using the Bio-Rad Protein Assay System (BioRad, Hertfordshire, UK) and the Bright-Glo™ Luciferase Assay System (Promega) respectively, according to manufacturer's protocol. Luminescence values were determined using a FLUOSTAR OPTIMA microplate reader (BMG LABTECH, Aylesbury, UK). Luminescence data of each sample were normalized to protein content (luciferase/μg).

Organotypic cultures

NTERT, SINCE and SINEG2 cells were grown with dermal human fibroblasts in organotypic 3D cultures, under conditions that support the proliferation and differentiation of epidermal keratinocytes and mimic their *in vivo* pattern of growth and differentiation. Briefly, collagen gels were prepared by mixing 7 volumes of collagen/matrigel (75% Collagen type I and 25% Matrigel, BD Bioscience) with 1 volume 10× DMEM (Invitogen, Paisley, UK), 1 volume FCS (Biosera), and 1 volume FGM in which HFF had been suspended at a concentration of 5×10^6/ml. Then 1ml of this solution (0.5×10^6 HFF) was aliquoted into wells of a 24-well plate and allowed to polymerise for 30 min at 37 ◦C. After polymerization, 1ml of FGM was added per well and gels were left for 18 h at 37◦C to equilibrate or $0.5x10^6$ of either N/TERT or SINCE or SINEG2 keratinocytes suspended

in 1ml of RM+ growth medium were seeded on top of each collagen gel. After 24h, gels were removed from the 24-well plates and placed on to individual collagen coated nylon discs resting on steel grids placed in six-well plates. Sufficient RM+ growth medium was added to reach the lower surface of the grid allowing the epithelial layer to grow at an air-liquid interface. Medium was changed every 2 days. Gels were harvested at day 14 and day 28 and fixed in 4% formaldehyde (Sigma) overnight. The organotypic cultures were bisected vertically and embedded in paraffin wax on their cut surface for sectioning. 4μm sections were cut from the organotypic cultures paraffin blocks and transferred to charged microscope slides for H&E or immuno- staining, to determine the invasion index, protein expression, as well as any phenotypic changes. Organotypic culture processing (wax embedding), sectioning, and H&E staining were all occurred at the Pathology Department of the Institute of Cancer, Barts and the London School of Medicine and Dentistry, Charterhouse square, London, UK. The H&E stained slides were imaged on the NanoZoomer Digital Pathology (NDP) whole slide scanner (Hamamatsu Photonics UK Limited, Hertfotdsire, UK), in brightfield mode and images were processed and analyzed using the Viewing Software NDP.view2 U12388-01.

Cytokeratin Immnunofluorescence in organotypic cultures

Briefly, paraffin embedded organotypic raft sections were initially heated at 60°C for 10 minutes and were then deparaffinised in Xylene (2×5 minutes) and dehydrated (100% ethanol (2x), 90% ethanol, 70% ethanol, 50% ethanol for 5 minutes each) prior to rehydrated in distilled water (5 minutes). Antigen unmasking was performed by incubation in sub-boiling temperature for 20 minutes in antigen retrieval solution (pH 6.0;

DakoCytomation). The sections were washed twice in PBS and blocked by 5% goat serum (Sigma) in PBS (PAA) with 0.05% Tween-20 (T) (Sigma) and 0.1% BSA (PAA) for 1 hour at room temperature (RT). Incubation with primary antibody in 1x PBS/0.05% T/0.1% BSA was performed for 2 hours at RT or overnight at 4°C. Sections were washed 3x5 minutes in 1x PBS/T, prior to incubation with Alexa Fluor 568 goat anti-mouse IgG (H+L) secondary antibody (Invitrogen) at 1:500 dilution in 1x PBS/0.05% T/0.1% BSA, for 1 hour at RT. Finally, sections were washed 3x5 minutes in 1x PBS/T and mounted with Prolong Gold Antifade Reagent Solution containing DAPI dilactate (Invitrogen).

Sectioning and Immunohistochemistry analysis in 3D cultures

Sectioning, immunostaining and imaging were performed at the Blizard Core Pathology Department, Queen Mary University of London, according to local standard protocols. Briefly, immunohistochemistry was carried out on 4µm sections (cut from the organotypic cultures processed in paraffin blocks) that were mounted on electrically charged slides (VWR, Leicestershire, UK) and dried overnight in a 60°C oven. The sections were stained on a DAKO Autostainer with the DAKO Flex+ Envision high pH Kit (K8012, DakoCytomation). The sections were antigen retrieved in the DAKO link machine (using the high pH from the kit above and at the factory settings) and then stained on the DAKO autostainer where the slides are treated with H_2O_2, primary antibody, linker, polymer secondary and visualised with DAB; all components (except primary antibodies) are from the kit and used at the times recommended. The sections were then counterstained with Gills Haematoxylin (In house preparation), dehydrated and cleared on a Gemini

Autostainer (Thermo Fisher, Leicestershire, UK) and cover-slipped with a xylene based mountant.

Supplementary Results

Generation and characterization of the inducible NTEG2 cell line

The preparation of the inducible cell line NTEG2 was based on the RevTet-OFF regulatory system, which allows efficient and tight quantitative and temporal control of gene expression. With this inducible system the transcription of the gene of interest (in this study EGFP-GLI2ΔN fusion gene) is turned off in the presence of doxycycline (Dox) (NTEG2 Dox+), while transcription of this gene (EGFP-GLI2ΔN fusion gene) is turned on in the absence of doxycycline (NTEG2 Dox-) (Supplementary Figure S2a). For the generation of the NTEG2 cell line we used heterogeneous cell populations in order to avoid any clone specific effects. Following drug selection and induction, NTEG2 cells were FACS sorted, and all EGFP+ cells were collected using N/TERT as a reference cell line to obtain baseline values of green fluorescence, replated and cultured under the presence of doxycycline.

Significant induction of protein levels was evidenced under fluorescent microscopy, 5 days after Dox removal (Supplementary Figure S2b; Dox(-) panels), while no induction of EGFP-GLI2ΔN fusion protein was observed in NTEG2 cells under the presence of doxycycline (Supplementary Figure S2b; Dox(+) panel). Flow cytometry analysis of NTEG2 cells showed an increased percentage of EGFP+ cells when Dox was removed, but also a small baseline induction of fluorescence even in Dox treated cells (Supplementary Figure S2c). Immunoblotting for EGFP-GLI2ΔN fusion protein confirmed GLI2ΔN induction in NTEG2 cells upon removal of Dox in comparison with baseline leak (Supplementary Figure S2d). Because we used pooled (FACS sorted EGFP+) NTEG2 cells, variation was observed in the levels of GLI2ΔN expression (EGFP intensity) between

different clones in NTEG2 culture (Supplementary Figure S2b compare the two lower Dox(-) panels). To control for this variation we always measured levels of EGFP-GLI2ΔN induction/suppression by flow cytometry and immunoblotting prior to carrying out experiments to ensure similar levels of GLI2ΔN expression between experiments.

Supplementary Figure Legends

Figure S1. Cyclin-D1 expression in GLI2ΔN-expressing keratinocytes. RNA was harvested from N/TERT, SINCE, and SINEG2 cells to examine the levels of Cyclin-D1 mRNA expression. Quantitative RT-PCR analysis showed an increase in the expression of Cyclin-D1 in SINEG2 cells compared to N/TERT and SINCE control cells. Each bar represents a mean ± s.e.m of triplicate samples. * $P \leq 0.05$, ** $P \leq 0.01$.

Figure S2. Generation and characterization of NTEG2 inducible cell line. (a) Diagram illustrating the principle of induction and/or repression of EGFP-GLI2ΔN fusion protein under the control of Doxycycline. Tetracycline controlled transactivator (tTa) binds to tetracycline response element (TRE) to activate transgene transcription mediated by the CMV promoter in the absence of doxycycline. tTa binding is repressed in the presence of doxycycline. **(b)** Representative pictures of NTEG2 cells in the presence (Dox(+)) or absence (Dox(-)) of doxycycline. Varying levels of EGFP-GLI2ΔN expression were observed possibly due to the heterogeneity of NTEG2 cell population. **(c)** Flow cytometry analysis of NTEG2 cell line in the presence or absence of doxycycline. Clear induction of EGFP-GLI2ΔN is shown in Dox(-) cells while background activity of EGFP-GLI2ΔN is also evidenced in the presence of doxycycline (top panel; Q2 quartile) represented by the small population detected above threshold levels of fluorescence obtained from wild-type N/TERT cells. **(d)** Immunoblotting analysis of NTEG2 cells in the presence or absence (5 days) of doxycycline against anti-EGFP antibody (EGFP-GLI2ΔN fusion protein ~ 180kDa), with β-actin (~ 42kDa) used as loading control. Significant induction of the

transgene is observed in Dox(-) cells, while background levels of induction are also present, as evidenced by previous flow cytometry analysis.

Figure S3. GLI2ΔN induces β-catenin transcriptional activation. (a) Immunoblotting in NTEG2 inducible cell line against EGFP antibody (EGFP-GLI2ΔN fusion protein ~180kDa), in the presence or absence of doxycycline, for 48h. β-actin (~42kDa) was used as loading control. Results indicated high levels of EGFP-GLI2ΔN fusion protein inducibility before the experiment. 48h of doxycycline withdrawal was the time-point of choice in order to achieve significant induction of EGFP-GLI2ΔN and maximum expression of SIN-OT-Luc reporter vector. **(b)** Luciferase assay on N/TERT and NTEG2 induced and uninduced cells. N/TERT keratinocytes were used as internal controls, due to background levels of GLI2ΔN in Dox+ NTEG2 cells. N/TERT and NTEG2 cells were transduced with SIN-OT-Luciferase vector and expressed the transgene for 72h, followed by doxycycline removal for another 48h. Day 5 post-transduction, lysates were prepared and examined for luciferase activity and protein content. OT-β-catenin responsive promoter was significantly activated in NTEG2 Dox- cells (~ 2.4 fold) compared to both N/TERT (*** $P \leq 0.001$) and NTEG2 Dox+ (** $P \leq 0.01$) cells. The increase in luciferase activity observed in uninduced NTEG2 cells (NTEG2 Dox+), compared to N/TERT cells can possibly be attributed to incomplete repression of GLI2ΔN in the presence of Dox. Each bar represents a mean ± s.e.m of normalised to protein content triplicate samples. **(c)** Active (dephosphorylated) β-catenin levels are increased in induced NTEG2 cells compared to the uninduced control cells. Active β-catenin levels in cell lysates from induced and uninduced NTEG2 cells were analysed by immunoblotting with anti-active-

β-catenin antibody (~92kDa). The EGFP-GLI2ΔN protein levels after 48h removal of doxycycline are also shown for reference and β-actin was used as loading control.

Figure S4. MMP2 expression in GLI2ΔN-expressing keratinocytes. (a) RNA was harvested from N/TERT, SINCE, and SINEG2 cells to examine the levels of MMP2 mRNA expression. qRT-PCR analysis showed an increase in the expression of MMP2 in SINEG2 cells compared to N/TERT and SINCE control cells. Each bar represents mean fold induction relative to N/TERT (arbitrary value of 1) ± s.e.m of triplicate samples.** $P \leq 0.01$. **(b)** Immuno-histochemical staining for MMP2 in sections of organotypic cultures of control SINCE cells (top panel) and SINEG2 cells (lower two panels) grown in collagen/matrigel gels for 14 days. Increased MMP2 expression is seen in SINEG2 cells compared to SINCE control cells, and shows a more pronounced staining in the edges/periphery of the invading multicellular strands with a bud-like tip (blue arrow) and clusters (red arrow). Scale bar: 100μm.

Figure S5. sFRP-1 blocks invasion of SINEG2 cells. 14-days organotypic cultures of SINEG2 cells treated with vehicle (top panel) or 0.1 μg/ml sFRP-1 (bottom panel). SIENG2 cells produce a thick basal-like undifferentiated epithelium in both conditions. When treated with vehicle only (top panel), SINEG2 cells display significant invasion capacity with clusters of cells invading the tissue, whereas treatment with sFRP-1 (bottom panel) reduces the capacity of SINEG2 cells to detach from the main bulk of the epithelium and invade into the organotypic ECM.

References

Chang YW, Jakobi R, McGinty A, Foschi M, Dunn MJ, Sorokin A. Cyclooxygenase 2 promotes cell survival by stimulation of dynein light chain expression and inhibition of neuronal nitric oxide synthase activity. Molecular and cellular biology. 2000;20:8571-9.

Chi TY, Chen GG, Ho LK, Lai PB. Establishment of a doxycycline-regulated cell line with inducible, doubly-stable expression of the wild-type p53 gene from p53-deleted hepatocellular carcinoma cells. Cancer cell international. 2005;5:27.

Deng H, Lin Q, Khavari PA. Sustainable cutaneous gene delivery. Nature biotechnology. 1997;15:1388-91.

Gemenetzidis E, Bose A, Riaz AM, Chaplin T, Young BD, Ali M, et al. FOXM1 upregulation is an early event in human squamous cell carcinoma and it is enhanced by nicotine during malignant transformation. PLoS ONE. 2009;4:e4849.

He TC, Sparks AB, Rago C, Hermeking H, Zawel L, da Costa LT, et al. Identification of c-MYC as a target of the APC pathway. Science (New York, NY. 1998;281:1509-12.

Korinek V, Barker N, Morin PJ, van Wichen D, de Weger R, Kinzler KW, et al. Constitutive transcriptional activation by a beta-catenin-Tcf complex in APC-/- colon carcinoma. Science (New York, NY. 1997;275:1784-7.

Pantazi E, Gemenetzidis E, Trigiante G, Warnes G, Shan L, Mao X, et al. GLI2 induces genomic instability in human keratinocytes by inhibiting apoptosis. Cell death & disease. 2014;5:e1028.

Shih IM, Yu J, He TC, Vogelstein B, Kinzler KW. The beta-catenin binding domain of adenomatous polyposis coli is sufficient for tumor suppression. Cancer research. 2000;60:1671-6.